ЖЭТФ, 2003, том 124, вып. 3 (9), стр. 491–515

NONLINEAR $k_\perp$-FACTORIZATION FOR FORWARD DIJETS IN DEEP INELASTIC SCATTERING OFF NUCLEI IN THE SATURATION REGIME

N. N. Nikolaev[a,b*], *W. Schäfer*[a], *B. G. Zakharov*[b], *V. R. Zoller*[c]

[a] *Institut für Kernphysik, Forschungszentrum Jülich D-52425, Jülich, Germany*

[b] *Landau Institute for Theoretical Physics 142432, Chernogolovka, Moscow Region, Russia*

[c] *Institute for Theoretical and Experimental Physics 117259, Moscow, Russia*

Submitted 11 March 2003

We develop a QCD description of the breakup of photons into forward dijets in small-x deep inelastic scattering off nuclei in the saturation regime. Based on the color dipole approach, we derive a multiple scattering expansion for intranuclear distortions of the jet–jet transverse momentum spectrum. A special attention is paid to the non-Abelian aspects of the propagation of color dipoles in the nuclear medium. We report a nonlinear $k_\perp$-factorization formula for the breakup of photons into dijets in terms of the collective Weizsäcker–Williams glue of nuclei defined in [5, 6]. For hard dijets with the transverse momenta above the saturation scale, the azimuthal decorrelation (acoplanarity) momentum is of the order of the nuclear saturation momentum Q_A. For minijets with the transverse momentum below the saturation scale, the nonlinear $k_\perp$-factorization predicts a complete disappearance of the jet–jet correlation. We comment on a possible relevance of the nuclear decorrelation of jets to the experimental data from the STAR-RHIC Collaboration.

PACS: 12.38.Aw, 13.87.Ce, 24.85.+p, 25.75.Gz

1. INTRODUCTION

From the parton model point of view, the opacity of heavy nuclei to high-energy projectiles entails a highly nonlinear relation between the parton densities of free nucleons and nuclei. The trademark of the conventional pQCD factorization theorems for hard interactions of leptons and hadrons is that the hard scattering observables are linear functionals of the appropriate parton densities in the projectile and target [1]. The parton model interpretation of hard phenomena in ultrarelativistic heavy ion collisions calls upon the understanding of factorization properties in the nonlinear regime. A priori, it is not obvious that nuclear parton densities can be defined such that they enter different observables in a universal manner. Indeed, opacity of nuclei brings in a new large scale Q_A that separates the regimes of opaque nuclei and weak attenuation [2–5]. Furthermore, for parton momenta below the saturation scale Q_A, the evolution of sea from gluons was shown to be dominated by the anticollinear, anti-DGLAP splitting [5]. In our early studies [5, 6], we have demonstrated that such observables as the amplitude of the coherent hard diffractive breakup of a projectile on a nucleus or the transverse momentum distribution of forward quark and antiquark jets in deep inelastic scattering (DIS) off a nucleus and/or the sea parton density of nuclei can be cast in precisely the same $k_\perp$-factorization form as for a free nucleon target. Specifically, this only requires replacing the unintegrated gluon structure function (SF) of the free nucleon with the collective nuclear Weizsäcker–Williams (WW) unintegrated nuclear glue, which is the expansion over the collective gluon SF of spatially overlapping nucleons of a Lorentz-contracted ultrarelativistic nucleus. This exact correspondence between the BFKL

*E-mail: N.Nikolaev@fz-juelich.de

unintegrated glue of the free nucleon [7] and the nonlinear collective WW glue of the nucleus in the calculation of these observables is a heartening finding. It persists despite the sea quarks and antiquarks with the transverse momenta below Q_A being generated by the anticollinear, anti-DGLAP splitting of gluons into sea, when the transverse momentum of the parent gluons is larger than the momentum of the produced sea quarks.

In [5], we noticed that less inclusive quantities like the spectrum of leading quarks from the truly inelastic DIS or coherent diffractive breakup off nuclei are nonlinear functionals of the collective nuclear WW glue. Consequently, in the quest for factorization properties of nuclear interactions, we must go beyond the one-parton observables such as the amplitude of coherent diffractive breakup of pions or photons into back-to-back dijets, single-jet inclusive cross section, and/or nuclear sea parton density. In this paper, we discuss the truly inelastic hard interaction with nuclei followed by a breakup of the projectile into forward hard dijets[1)]. We illustrate our major point in the example of DIS at small x with a breakup of the (virtual) photon into a hard approximately back-to-back dijet with a small separation in rapidity, such that the so-called lightcone plus-components of the jet momenta sum up to the lightcone plus-component of the photon momentum, i.e., the so-called $x_\gamma = 1$ criterion is fulfilled (see, e.g., [10] and references therein). In the familiar collinear approximation, such a dijet originates from the photon–gluon fusion $\gamma^* g \to q\bar{q}$, often referred to as the interaction of the unresolved or direct photon. Allowing a transverse momentum of gluons leads to a disparity of the momenta and to an azimuthal decorrelation of the quark and antiquark jets, which can be quantified in DIS off free protons within the $k_\perp$-factorization in terms of the unintegrated gluon SF of the target (see [11, 12] and references therein). A substantial nuclear broadening of the unintegrated gluon SF of nuclei at small x and of the nuclear sea parton distributions [2, 5] points at a stronger azimuthal decorrelation of jets produced in DIS off nuclei. Furthermore, our finding of anticollinear, anti-DGLAP splitting of gluons into sea strongly suggests the complete azimuthal decorrelation of forward quark and antiquark jets with the transverse momenta below the saturation scale, $p_\pm \lesssim Q_A$. In this paper, we quantify these expectations and formulate a nonlinear generalization of the $k_\perp$-factorization for the inclusive dijet spectrum.

The technical basis of our approach is the color-dipole multiple-scattering theory of small-x DIS off nuclei [13, 14]. We derive a consistent $k_\perp$-factorization description of the azimuthal decorrelation of jets in terms of the collective WW unintegrated gluon SF of the nucleus. In this derivation, we closely follow our early work [5] on the color-dipole approach to saturation of nuclear partons. We focus on DIS at $x \lesssim x_A = 1/R_A m_N \ll 1$, which is dominated by interactions of $q\bar{q}$ Fock states of the photon. Here, m_N is the nucleon mass and R_A is the radius of the target nucleus of the mass number A. Nuclear attenuation of these $q\bar{q}$ color dipoles [13, 15] quantifies the fusion of gluons and sea quarks from spatially overlapping nucleons of the Lorentz contracted nucleus ([16], also see [3, 4]). Here, we also report some of the technical details, especially on the non-Abelian aspects of propagation of color dipoles in nuclear matter, which were omitted in the letter publication [5].

We focus on the genuinely inelastic DIS followed by color excitation of the target nucleus. For heavy nuclei, equally important is the coherent diffractive DIS in which the target nucleus does not break and is retained in the ground state. Coherent diffractive DIS makes 50 % of the total DIS events at small x [14]; in these coherent diffractive events, quark and antiquark jets are produced exactly back-to-back with a negligibly small transverse decorrelation momentum $|\mathbf{\Delta}| = |\mathbf{p}_+ + \mathbf{p}_-| \lesssim 1/R_A \sim m_\pi/A^{1/3}$.

This paper is organized as follows. We work at the parton level and discuss the transverse momentum distribution of the final state quark and antiquark in interactions of $q\bar{q}$ Fock states of the photon with heavy nuclei. In Sec. 2, we set up the formalism with a brief discussion of the decorrelation of jets in DIS off free nucleons. In Sec. 3, we report the derivation of the general formula for the two-body transverse momentum distribution. Color exchange between the initially color-neutral $q\bar{q}$ dipole and the nucleons of the target nucleus leads to intranuclear propagation of the color-octet $q\bar{q}$-states. Our formalism, based on the technique described in [17, 18], consistently includes the diffractive attenuation of octet dipoles and effects of transitions between color-singlet and color-octet $q\bar{q}$ pairs, as well as between different color states of the $q\bar{q}$ pair. The hard jet–jet inclusive cross section is discussed in Sec. 4. For hard dijets, diffractive attenuation effects are weak, and we obtain a nuclear $k_\perp$-factorizaton formula for the broadening of azimuthal correlations between the quark and antiquark jets, which is reminiscent of that for a free nucleon target and is still a linear functional of the collective WW gluon SF of the nucleus. We relate the decorrelation (acoplanarity) momentum to the

[1)] Preliminary results of this study have been reported elsewhere [8, 9].

nuclear saturation scale Q_A. In Sec. 5, working in the large-N_c approximation, we derive our central result, a nonlinear nuclear $k_\perp$-factorization formula for the inclusive dijet cross section, and prove the complete disappearance of the jet–jet correlation for minijets with the transverse momentum below the saturation scale Q_A. In Sec. 6, we present numerical estimates for the acoplanarity momentum distribution based on the unintegrated glue of the proton determined in [19]. We point out a strong enhancement of decorrelations from the average to central DIS and comment on possible relevance of our mechanism of azimuthal decorrelations to the recent observation of the dissolution of the away jets in central nuclear collisions at RHIC [20]. The next-to-leading order $1/N_c^2$-corrections to the large-N_c results in Sec. 5 are discussed in Sec. 7. Here, we derive a nonlinear $k_\perp$-factorization representation for the $1/N_c^2$ corrections and establish a close connection between the $1/N_c^2$ and higher-twist expansions. In Sec. 8, we summarize our principal findings.

Some of the technical details are presented in the Appendices. In Appendix A, we present the calculation of the matrix of 4-body cross sections that enters the evolution operator for the intranuclear propagation of color dipoles. In Appendix B, we revisit the single-jet spectrum and total cross section of DIS off nuclei and demonstrate how the color-dipole extension [13, 14] of the Glauber–Gribov results [21, 22] is recovered despite a nontrivial spectrum of eigen-cross sections for the non-Abelian propagation of color dipoles in the nuclear matter. The properties of the collective unintegrated gluon SF for overlapping nucleons of a Lorentz-contracted ultrarelativistic nucleus are discussed in Appendix C.

2. $K_\perp$-FACTORIZATION FOR BREAKUP OF PHOTONS INTO FORWARD DIJETS IN DIS OFF FREE NUCLEONS

We briefly recall the color dipole formulation of DIS [13, 14, 23–25] and set up the formalism in the example of jet–jet decorrelation in DIS off free nucleons at moderately small x, which is dominated by interactions of $q\bar{q}$ states of the photon. The total cross section for the interaction of the color dipole $\mathbf{r}$ with the target nucleon is given by [26, 27]

$$\sigma(r) = \alpha_S(r)\sigma_0 \int d\boldsymbol{\kappa} f(\boldsymbol{\kappa}) \left(1 - e^{i\boldsymbol{\kappa}\cdot\mathbf{r}}\right) = \\ = \frac{1}{2}\alpha_S(r)\sigma_0 \int d\boldsymbol{\kappa} f(\boldsymbol{\kappa}) \left(1 - e^{i\boldsymbol{\kappa}\cdot\mathbf{r}}\right)\left(1 - e^{-i\boldsymbol{\kappa}\cdot\mathbf{r}}\right), \quad (1)$$

where σ_0 is an auxiliary soft parameter and α_S is the running coupling constant for the gauge group $SU(N_c)$. The function $f(\boldsymbol{\kappa})$ is normalized as $\int d\boldsymbol{\kappa} f(\boldsymbol{\kappa}) = 1$, α_S is a running coupling constant for the gauge group $SU(N_c)$, related to the BFKL unintegrated gluon SF of the target nucleon $\mathcal{F}(x,\kappa^2) = \partial G(x,\kappa^2)/\partial \ln \kappa^2$ ([7], also see [19, 28] for the phenomenology and review) by

$$f(\boldsymbol{\kappa}) = \frac{4\pi}{N_c\sigma_0}\,\frac{1}{\kappa^4}\,\mathcal{F}(x,\kappa^2). \quad (2)$$

For DIS off a free nucleon target (see Figs. 1*a–d*), the total photoabsorption cross section is given by [13]

$$\sigma_N(Q^2,x) = \int d\mathbf{r}\, dz |\Psi(Q^2,z,\mathbf{r})|^2 \sigma(x,\mathbf{r}), \quad (3)$$

where $\Psi(Q^2,z,\mathbf{r})$ is the wave function of the $q\bar{q}$ Fock state of the photon and Q^2 and x are the standard DIS variables. In the momentum representation,

$$\frac{d\sigma_N}{d\mathbf{p}_+\, dz} = \frac{\sigma_0}{2}\,\frac{\alpha_S(\mathbf{p}_+^2)}{(2\pi)^2} \times \\ \times \int d\boldsymbol{\kappa} f(\boldsymbol{\kappa}) \left|\langle\gamma^*|z,\mathbf{p}_+\rangle - \langle\gamma^*|z,\mathbf{p}_+ - \boldsymbol{\kappa}\rangle\right|^2, \quad (4)$$

where $\mathbf{p}_+$ is the transverse momentum of the quark, the antiquark has the transverse momentum $\mathbf{p}_- = -\mathbf{p}_+ + \boldsymbol{\kappa}$, and $z_+ = z$ and $z_- = 1 - z$ are the fractions of the photon lightcone momentum carried by the quark and antiquark, respectively. The variables $z_\pm$ for the observed jets add up to unity, $x_\gamma = z_+ + z_- = 1$, which in the realm of DIS is said to be the unresolved (or direct) photon interaction.

Summing over the helicities λ and $\overline{\lambda}$ of the final state quark and antiquark, we obtain

$$\left|\langle\gamma^*|z,\mathbf{p}\rangle - \langle\gamma^*|z,\mathbf{p}-\boldsymbol{\kappa}\rangle\right|^2_{\lambda_\gamma=\pm1} = 2N_c e_f^2 \alpha_{em} \times \\ \times \left\{ [z^2+(1-z)^2] \left(\frac{\mathbf{p}}{\mathbf{p}^2+\varepsilon^2} - \frac{\mathbf{p}-\boldsymbol{\kappa}}{(\mathbf{p}-\boldsymbol{\kappa})^2+\varepsilon^2}\right)^2_{\lambda+\overline{\lambda}=0} + \right. \\ \left. + m_f^2 \left(\frac{1}{\mathbf{p}^2+\varepsilon^2} - \frac{1}{(\mathbf{p}-\boldsymbol{\kappa})^2+\varepsilon^2}\right)^2_{\lambda+\overline{\lambda}=\lambda_\gamma} \right\} \quad (5)$$

for transverse photons and quarks of flavor f and

$$\left|\langle\gamma^*|z,\mathbf{p}\rangle - \langle\gamma^*|z,\mathbf{p}-\boldsymbol{\kappa}\rangle\right|^2_{\lambda_\gamma=0} = \\ = 8N_c e_f^2 \alpha_{em} Q^2 z^2 (1-z)^2 \times \\ \times \left(\frac{1}{\mathbf{p}^2+\varepsilon^2} - \frac{1}{(\mathbf{p}-\boldsymbol{\kappa})^2+\varepsilon^2}\right)^2_{\lambda+\overline{\lambda}=\lambda_\gamma} \quad (6)$$

for longitudinal photons, where $\varepsilon^2 = z(1-z)Q^2 + m_f^2$.

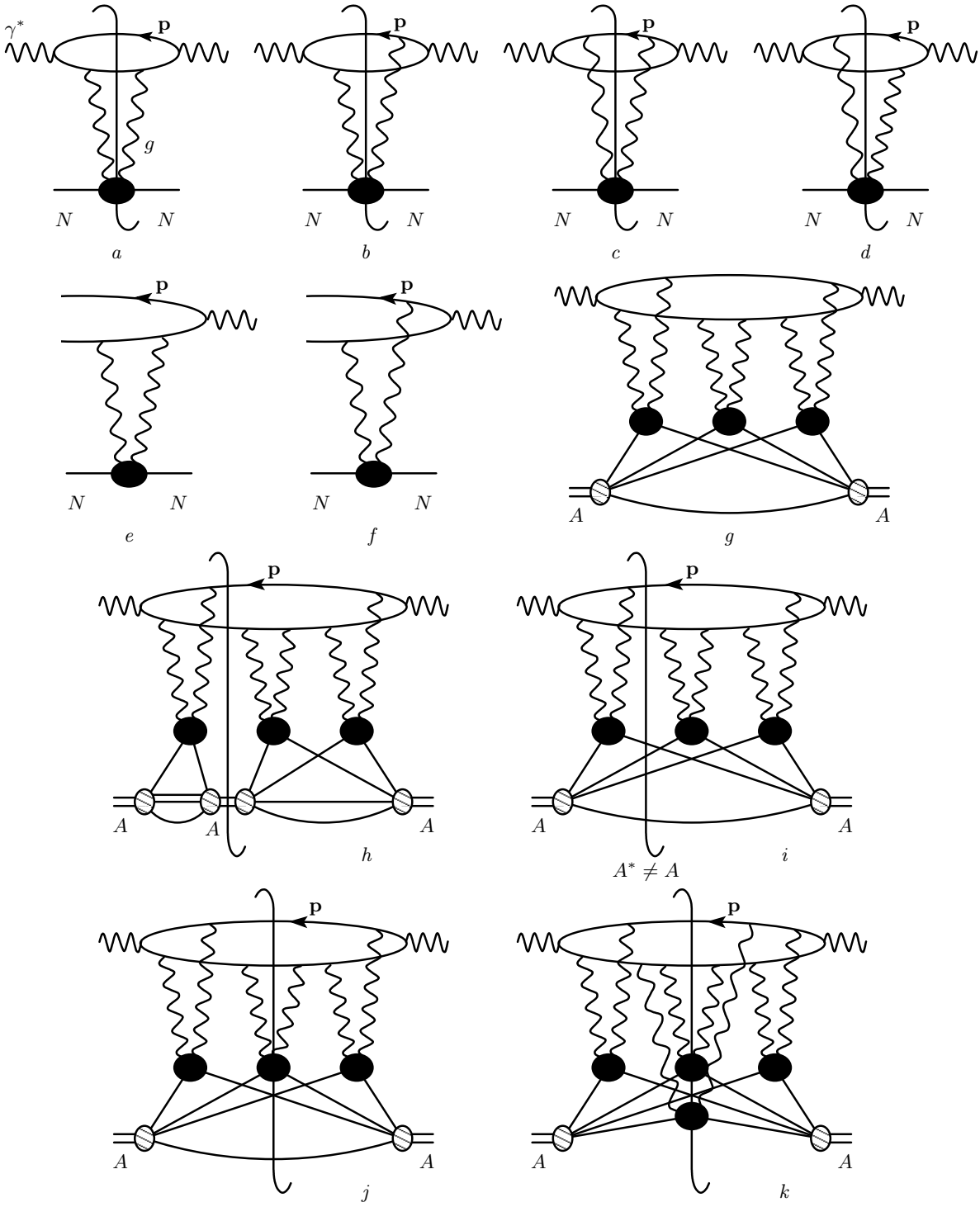

Fig. 1. pQCD diagrams for the cross section of inclusive DIS off nucleons (a–d) and nuclei (g–k) and the amplitude of diffractive DIS off protons (e, f). Diagrams a–d show the unitarity cuts with color excitation of the target nucleon, g is a generic multiple scattering diagram for the Compton scattering amplitude off nucleus, h is the unitarity cut for a coherent diffractive DIS with retention of the ground state nucleus A in the final state, i is the unitarity cut for quasielastic diffractive DIS with excitation and breakup of the nucleus A^*, j and k are the unitarity cuts for truly inelastic DIS with single (j) and multiple (k) color excitation of nucleons of the nucleus

We now note that the transverse momentum of the gluon is precisely the decorrelation momentum $\mathbf{\Delta} = \mathbf{p}_+ + \mathbf{p}_-$, and in the differential form, we have

$$\frac{d\sigma_N}{dz\, d\mathbf{p}_+ d\mathbf{\Delta}} = \frac{\sigma_0}{2}\frac{\alpha_S(\mathbf{p}_+^2)}{(2\pi)^2} f(\mathbf{\Delta}) \times \\ \times |\langle\gamma^*|z,\mathbf{p}_+\rangle - \langle\gamma^*|z,\mathbf{p}_+ - \mathbf{\Delta}\rangle|^2 = \\ = \frac{\alpha_S(\mathbf{p}_+^2)}{2\pi N_c}\frac{\mathcal{F}(x,\mathbf{\Delta}^2)}{\Delta^4} \times \\ \times |\langle\gamma^*|z,\mathbf{p}_+\rangle - \langle\gamma^*|z,\mathbf{p}_+ - \mathbf{\Delta}\rangle|^2. \quad (7)$$

The small-x result in Eq. (7) shows that in DIS, forward dijets acquire their large transverse momentum from the intrinsic momentum of the quark and antiquark in the wave function of the projectile photon; hence, it is appropriate to call this process the breakup of the photon into forward hard dijets. In addition to the criterion $x_\gamma = 1$, the experimental signature of the photon breakup is a small rapidity separation of forward jets, $z_+ \sim z_-$. The perturbative hard scale for our process is set by $Q_h^2 = 4\mathbf{p}_+^2 + Q^2$ and the gluon SF of the proton enters Eq. (7) at the Bjorken variable $x = (4\mathbf{p}_+^2 + Q^2)/W^2$, where W is the $\gamma^* p$ center-of-mass energy. The purpose of our study is an extension of Eq. (7) to the breakup of photons into dijets in truly inelastic DIS on nuclear targets.

3. BREAKUP OF PHOTONS INTO DIJETS ON NUCLEAR TARGETS

We focus on DIS at $x \lesssim x_A = 1/R_A m_N \ll 1$, which is dominated by interactions of $q\bar{q}$ states of the photon. This is a starting term of the leading $\ln(1/x)$ expansion; extension to interactions of higher Fock states of the photon and the corresponding $\ln(1/x)$ evolution to smaller x will be discussed elsewhere. For $x \lesssim x_A$, the propagation of the $q\bar{q}$ pair inside the nucleus can be treated in the straight-path approximation.

We work in the conventional approximation of two t-channel gluons in DIS off free nucleons. The relevant unitarity cuts of the forward Compton scattering amplitude shown in Figs. 1*a–d* describe the transition from the color-neutral $q\bar{q}$ dipole to the color-octet $q\bar{q}$ pair[2)]. The two-gluon exchange approximation amounts to neglecting unitarity constraints in DIS off free nucleons. As a quantitative measure of unitarity corrections, one can take diffractive DIS off free nucleons, whose amplitude is described by higher-order diagrams in Figs. 1*e, f* [23, 24, 27] and which is only a small fraction of the total DIS, $\eta_D \ll 1$ [29–31]. The unitarity cuts of the nuclear Compton scattering amplitude that correspond to the genuine inelastic DIS with color excitation of the nucleus are shown in Figs. 1*j, k*. The diagram in Fig. 1*k* describes a consecutive color excitation of the target nucleus accompanied by the color-space rotation of the color-octet $q\bar{q}$.

Let $\mathbf{b}_+$ and $\mathbf{b}_-$ be the impact parameters of the quark and antiquark, respectively, and $S_A(\mathbf{b}_+,\mathbf{b}_-)$ be the S-matrix for the interaction of the $q\bar{q}$ pair with the nucleus. We are interested in the truly inelastic inclusive cross section summed over all excitations of the target nucleus when one or several nucleons are color excited. A convenient way to sum such cross sections is offered by the closure relation [21]. Regarding the color states c_{km} of the $q_k\bar{q}_m$ pair, we sum over all octet and singlet states. Then the 2-jet inclusive spectrum is calculated in terms of the 2-body density matrix as

$$\frac{d\sigma_{in}}{dz\, d\mathbf{p}_+ d\mathbf{p}_-} = \frac{1}{(2\pi)^4}\int d\mathbf{b}'_+ d\mathbf{b}'_- d\mathbf{b}_+ d\mathbf{b}_- \times \\ \times \exp[-i\mathbf{p}_+\cdot(\mathbf{b}_+ - \mathbf{b}'_+) - i\mathbf{p}_-\cdot(\mathbf{b}_- - \mathbf{b}'_-)] \times \\ \times \Psi^*(Q^2,z,\mathbf{b}'_+ - \mathbf{b}'_-)\Psi(Q^2,z,\mathbf{b}_+ - \mathbf{b}_-) \times \\ \times \Big\{\sum_{A^*}\sum_{km}\langle 1;A|S_A^*(\mathbf{b}'_+,\mathbf{b}'_-)|A^*;c_{km}\rangle \times \\ \times\langle c_{km};A^*|S_A(\mathbf{b}_+,\mathbf{b}_-)|A;1\rangle - \\ - \langle 1;A|S_A^*(\mathbf{b}'_+,\mathbf{b}'_-)|A;1\rangle\langle 1;A| \times \\ \times S_A(\mathbf{b}_+,\mathbf{b}_-)|A;1\rangle\Big\}. \quad (8)$$

In the integrand in Eq. (8), we subtracted the coherent diffractive component of the final state. We note that four straight-path trajectories $\mathbf{b}_\pm$ and $\mathbf{b}'_\pm$ enter the calculation of the full-fledged 2-body density matrix and S_A and S_A^* describe the propagation of two quark–antiquark pairs, $q\bar{q}$ and $q'\bar{q}'$, inside a nucleus.

The further analysis of the integrand in Eq. (8) is a non-Abelian generalization of the formalism developed by one of the authors (B. G. Z.) for the in-medium evolution of ultrarelativistic positronium [32]. Upon the application of the closure relation to sum over nuclear final states A^*, the integrand in Eq. (8) can be considered as an intranuclear evolution operator for the 2-body density matrix

[2)] To be more precise, for arbitrary N_c, the color-excited $q\bar{q}$ pair is in the adjoint representation and quarks are in the fundamental representation of $SU(N_c)$; our reference to the color octet and triplet must not cause any confusion.

$$\sum_{A^*}\sum_{km}\langle A|\Big\{\langle 1|S_A^*(\mathbf{b}'_+,\mathbf{b}'_-)|c_{km}\rangle\Big\}|A^*\rangle\times$$
$$\times\langle A^*|\Big\{\langle c_{km}|S_A(\mathbf{b}_+,\mathbf{b}_-)|1\rangle\Big\}|A\rangle=$$
$$=\langle A|\left\{\sum_{km}\langle 1|S_A^*(\mathbf{b}'_+,\mathbf{b}'_-)|c_{km}\rangle\times\right.$$
$$\left.\times\,\langle c_{km}|S_A(\mathbf{b}_+,\mathbf{b}_-)|1\rangle\right\}|A\rangle \quad (9)$$

(for the related discussion, also see Ref. [33]). Let the eikonal for the quark–nucleon and antiquark–nucleon QCD gluon exchange interaction be $T_+^a\chi(\mathbf{b})$ and $T_-^a\chi(\mathbf{b})$, where T_+^a and T_-^a are the $SU(N_c)$ generators for the quark and antiquark states, respectively. The vertex V_a for excitation of the nucleon, $g^aN\to N_a^*$, into the color octet state is normalized such that after application of the closure relation, the vertex g^ag^bNN in the diagrams in Figs. 1*a–d* becomes δ_{ab}. In the two-gluon exchange approximation, the S-matrix of the $(q\bar q)$–nucleon interaction is then given by

$$S_N(\mathbf{b}_+,\mathbf{b}_-)=1+i[T_+^a\chi(\mathbf{b}_+)+T_-^a\chi(\mathbf{b}_-)]V_a-$$
$$-\frac{1}{2}[T_+^a\chi(\mathbf{b}_+)+T_-^a\chi(\mathbf{b}_-)]^2. \quad (10)$$

The profile function for the interaction of the $q\bar q$ dipole with the nucleon is $\Gamma(\mathbf{b}_+,\mathbf{b}_-)=1-S_N(\mathbf{b}_+,\mathbf{b}_-)$. For a color-singlet dipole, $(T_+^a+T_-^a)^2=0$ and the dipole cross section for the interaction of the color-singlet $q\bar q$ dipole with the nucleon equals

$$\sigma(\mathbf{b}_+-\mathbf{b}_-)=2\int d\mathbf{b}_+\langle N|\Gamma(\mathbf{b}_+,\mathbf{b}_-)|N\rangle=$$
$$=\frac{N_c^2-1}{2N_c}\int d\mathbf{b}_+[\chi(\mathbf{b}_+)-\chi(\mathbf{b}_-)]^2. \quad (11)$$

The nuclear S-matrix of the straight-path approximation is

$$S_A(\mathbf{b}_+,\mathbf{b}_-)=\prod_{j=1}^{A}S_N(\mathbf{b}_+-\mathbf{b}_j,\mathbf{b}_--\mathbf{b}_j),$$

where the ordering along the longitudinal path is understood. We evaluate the nuclear expectation value in (9) in the standard dilute gas approximation. In the two-gluon exchange approximation, for each and every nucleon N_j, only the terms quadratic in $\chi(\mathbf{b}_j)$ must be kept in the single-nucleon matrix element

$$\langle N_j|S_N^*(\mathbf{b}'_+-\mathbf{b}_j,\mathbf{b}'_--\mathbf{b}_j)S_N(\mathbf{b}_+-\mathbf{b}_j,\mathbf{b}_--\mathbf{b}_j)|N_j\rangle$$

that enters the calculation of $S_A^*S_A$. Following the technique developed in [17, 18], we can reduce the calculation of the evolution operator for the 2-body density matrix (9) to the evaluation of the S-matrix $S_{4A}(\mathbf{b}_+,\mathbf{b}_-,\mathbf{b}'_+,\mathbf{b}'_-)$ for the scattering of a fictitious 4-parton state composed of the two quark–antiquark pairs in the overall color-singlet state. Because $(T_+^a)^*=-T_-^a$, the quarks entering the complex-conjugate S_A^* in (9) can be viewed as antiquarks within the two-gluon exchange approximation, and therefore

$$\sum_{km}\langle 1|S_A^*(\mathbf{b}'_+,\mathbf{b}'_-)|c_{km}\rangle\langle c_{km}|S_A(\mathbf{b}_+,\mathbf{b}_-)|1\rangle=$$
$$=\sum_{kmjl}\delta_{kl}\delta_{mj}\langle c_{km}c_{jl}|S_{4A}(\mathbf{b}'_+,\mathbf{b}'_-,\mathbf{b}_+,\mathbf{b}_-)|11\rangle, \quad (12)$$

where $S_{4A}(\mathbf{b}'_+,\mathbf{b}'_-,\mathbf{b}_+,\mathbf{b}_-)$ is the S-matrix for the propagation of two quark–antiquark pairs in the overall singlet state. While the first $q\bar q$ pair is formed by the initial quark q and antiquark $\bar q$ at the respective impact parameters $\mathbf{b}_+$ and $\mathbf{b}_-$, the quark q' in the second $q'\bar q'$ pair propagates at the impact parameter $\mathbf{b}'_-$ and the antiquark $\bar q'$ at the impact parameter $\mathbf{b}'_+$. In the initial state, both quark–antiquark pairs are in color-singlet states, $|in\rangle=|11\rangle$.

We introduce the normalized singlet–singlet and octet–octet states

$$|11\rangle=\frac{1}{N_c}(\bar qq)(\bar q'q'),$$
$$|88\rangle=\frac{2}{\sqrt{N_c^2-1}}(\bar qT^aq)(\bar q'T^aq'), \quad (13)$$

where N_c is the number of colors and T^a are the generators of $SU(N_c)$ in the fundamental representation. Using the color Fiertz identity,

$$\delta_j^k\delta_l^m=\frac{1}{N_c}\delta_l^k\delta_j^m+2\sum_a(T^a)_l^k(T^a)_j^m, \quad (14)$$

we can represent the sum (12) over color states of the produced quark–antiquark pair as

$$\sum_{km}\langle c_{km}c_{km}|S_{4A}(\mathbf{b}'_+,\mathbf{b}'_-,\mathbf{b}_+,\mathbf{b}_-)|11\rangle=$$
$$=\langle 11|S_{4A}(\mathbf{b}'_+,\mathbf{b}'_-,\mathbf{b}_+,\mathbf{b}_-)|11\rangle+$$
$$+\sqrt{N_c^2-1}\langle 88|S_{4A}(\mathbf{b}'_+,\mathbf{b}'_-,\mathbf{b}_+,\mathbf{b}_-)|11\rangle. \quad (15)$$

If $\sigma_4(\mathbf{b}'_+,\mathbf{b}'_-,\mathbf{b}_+,\mathbf{b}_-)$ is the color-dipole cross section operator for the 4-body state, evaluation of the nuclear expectation value for a dilute gas nucleus in the standard approximation of neglecting the size of color dipoles compared to the radius of a heavy nucleus gives [21]

$$S_{4A}(\mathbf{b}'_+,\mathbf{b}'_-,\mathbf{b}_+,\mathbf{b}_-)=$$
$$=\exp\left\{-\frac{1}{2}\sigma_4(\mathbf{b}'_+,\mathbf{b}'_-,\mathbf{b}_+,\mathbf{b}_-)T(\mathbf{b})\right\}, \quad (16)$$

where $T(\mathbf{b}) = \int db_z n_A(b_z, \mathbf{b})$ is the optical thickness of the nucleus at the impact parameter[3)]

$$\mathbf{b} = \frac{1}{4}(\mathbf{b}_+ + \mathbf{b}'_+ + \mathbf{b}_- + \mathbf{b}'_-)$$

and $n_A(b_z, \mathbf{b})$ is the nuclear matter density with the normalization $\int d\mathbf{b} T(\mathbf{b}) = A$. Single-nucleon S-matrix (10) contains transitions from the color-singlet to both color-singlet and color-octet $q\bar{q}$ pairs. However, only color-singlet operators contribute to

$$\langle N_j | S_N^*(\mathbf{b}'_+ - \mathbf{b}_j, \mathbf{b}'_- - \mathbf{b}_j) S_N(\mathbf{b}_+ - \mathbf{b}_j, \mathbf{b}_- - \mathbf{b}_j) | N_j \rangle,$$

and hence the matrix $\sigma_4(\mathbf{b}'_+, \mathbf{b}'_-, \mathbf{b}_+, \mathbf{b}_-)$ only includes transitions between the $|11\rangle$ and $|88\rangle$ color-singlet 4-parton states; the $|18\rangle$ states are not allowed.

The pQCD diagrams for the 4-body cross section are shown in Fig. 2. It is convenient to introduce

$$\mathbf{s} = \mathbf{b}_+ - \mathbf{b}'_+, \tag{17}$$

for the variable conjugate to the decorrelation momentum, and $\mathbf{r} = \mathbf{b}_+ - \mathbf{b}_-$, $\mathbf{r}' = \mathbf{b}'_+ - \mathbf{b}'_-$, in terms of which

$$\begin{aligned} \mathbf{b}_+ - \mathbf{b}'_- = \mathbf{s} + \mathbf{r}', \quad \mathbf{b}_- - \mathbf{b}'_+ = \mathbf{s} - \mathbf{r}, \\ \mathbf{b}_- - \mathbf{b}'_- = \mathbf{s} - \mathbf{r} + \mathbf{r}'. \end{aligned} \tag{18}$$

Performing the relevant color algebra, we find (some details of the derivation are presented in Appendix A)

$$\sigma_{11} = \langle 11 | \sigma_4 | 11 \rangle = \sigma(\mathbf{r}) + \sigma(\mathbf{r}'), \tag{19}$$

$$\begin{aligned} \sigma_{18} = \langle 11 | \sigma_4 | 88 \rangle = \\ = \frac{\sigma(\mathbf{s}) + \sigma(\mathbf{s} - \mathbf{r} + \mathbf{r}') - \sigma(\mathbf{s} + \mathbf{r}') - \sigma(\mathbf{s} - \mathbf{r})}{\sqrt{N_c^2 - 1}} = \\ = -\frac{\Sigma_{18}(\mathbf{s}, \mathbf{r}, \mathbf{r}')}{\sqrt{N_c^2 - 1}}, \end{aligned} \tag{20}$$

$$\begin{aligned} \sigma_{88} = \langle 88 | \sigma_4 | 88 \rangle = \frac{N_c^2 - 2}{N_c^2 - 1} [\sigma(\mathbf{s}) + \sigma(\mathbf{s} - \mathbf{r} + \mathbf{r}')] + \\ + \frac{2}{N_c^2 - 1} [\sigma(\mathbf{s} + \mathbf{r}') + \sigma(\mathbf{s} - \mathbf{r})] - \frac{1}{N_c^2 - 1} [\sigma(\mathbf{r}) + \sigma(\mathbf{r}')]. \end{aligned} \tag{21}$$

The term in (8) that subtracts the contribution from diffractive processes without color excitation of the target nucleus is given by

$$\begin{aligned} \langle 1; A | S_A^*(\mathbf{b}'_+, \mathbf{b}'_-) | A; 1 \rangle \langle 1; A | S_A(\mathbf{b}_+, \mathbf{b}_-) | A; 1 \rangle = \\ = \exp\left\{ -\frac{1}{2} [\sigma(\mathbf{r}) + \sigma(\mathbf{r}')] T(\mathbf{b}) \right\} = \\ = \exp\left\{ -\frac{1}{2} \sigma_{11} T(\mathbf{b}) \right\}. \end{aligned} \tag{22}$$

In the discussion of nuclear effects, it is convenient to use the Sylvester expansion

$$\begin{aligned} \exp\left\{ -\frac{1}{2} \sigma_4 T(\mathbf{b}) \right\} = \exp\left\{ -\frac{1}{2} \Sigma_1 T(\mathbf{b}) \right\} \frac{\sigma_4 - \Sigma_2}{\Sigma_1 - \Sigma_2} + \\ + \exp\left\{ -\frac{1}{2} \Sigma_2 T(\mathbf{b}) \right\} \frac{\sigma_4 - \Sigma_1}{\Sigma_2 - \Sigma_1}, \end{aligned} \tag{23}$$

where $\Sigma_{1,2}$ are the two eigenvalues of the operator σ_4,

$$\begin{aligned} \Sigma_{1,2} = \frac{1}{2}(\sigma_{11} + \sigma_{88}) \mp \\ \mp \frac{1}{2}(\sigma_{11} - \sigma_{88}) \sqrt{1 + \frac{4\sigma_{18}^2}{(\sigma_{11} - \sigma_{88})^2}}. \end{aligned} \tag{24}$$

For the integrand in (8), application of the Sylvester expansion to (15) gives

$$\begin{aligned} \sum_{A^*} \sum_{km} \langle 1; A | S_A^*(\mathbf{b}'_+, \mathbf{b}'_-) | A^*; c_{km} \rangle \times \\ \times \langle c_{km}; A^* | S_A(\mathbf{b}_+, \mathbf{b}_-) | A; 1 \rangle - \\ - \langle 1; A | S_A^*(\mathbf{b}'_+, \mathbf{b}'_-) | A; 1 \rangle \langle 1; A | S_A(\mathbf{b}_+, \mathbf{b}_-) | A; 1 \rangle = \\ = (\langle 11 | + \sqrt{N_c^2 - 1} \langle 88 |) \exp\left\{ -\frac{1}{2} \sigma_4 T(\mathbf{b}) \right\} | 11 \rangle - \\ - \exp\left\{ -\frac{1}{2} \sigma_{11} T(\mathbf{b}) \right\} = \\ = \exp\left\{ -\frac{1}{2} \Sigma_2 T(\mathbf{b}) \right\} - \exp\left\{ -\frac{1}{2} \sigma_{11} T(\mathbf{b}) \right\} + \\ + \frac{\sigma_{11} - \Sigma_2}{\Sigma_1 - \Sigma_2} \left\{ \exp\left[-\frac{1}{2} \Sigma_1 T(\mathbf{b}) \right] - \exp\left[-\frac{1}{2} \Sigma_2 T(\mathbf{b}) \right] \right\} + \\ + \frac{\sqrt{N_c^2 - 1} \sigma_{18}}{\Sigma_1 - \Sigma_2} \left\{ \exp\left[-\frac{1}{2} \Sigma_1 T(\mathbf{b}) \right] - \right. \\ \left. - \exp\left[-\frac{1}{2} \Sigma_2 T(\mathbf{b}) \right] \right\}. \end{aligned} \tag{25}$$

4. BREAKING OF PHOTONS INTO HARD DIJETS: A STILL LINEAR NUCLEAR $k_\perp$-FACTORIZATION

Diagonalization of the 2×2 matrix σ_4 is a straightforward task, and therefore technically, Eqs. (8) and

[3)] One should not confuse $\mathbf{b}$ with the center of gravity of color dipoles, where the impact parameters $\mathbf{b}_\pm$ and $\mathbf{b}'_\pm$ must be weighted with $z_\pm$; the difference between the two quantities is irrelevant here.

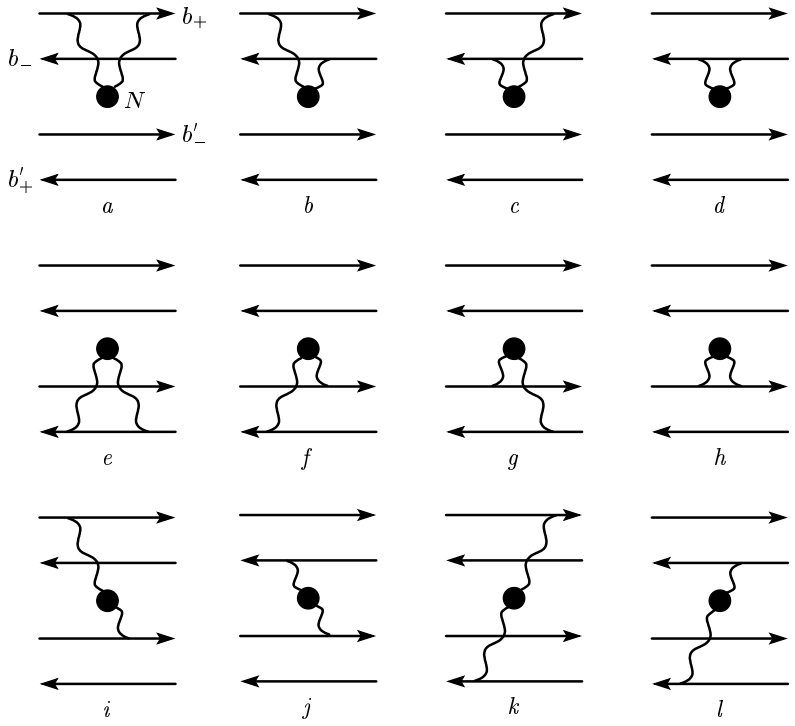

Fig. 2. The pQCD diagrams for the matrix of color dipole cross section for the 4-body $(q\bar{q})(q'\bar{q}')$ state. The sets a–d and e–h show the diagrams for the scattering without changing the color state of the $q\bar{q}$ and $q'\bar{q}'$ dipoles, the set i–l shows only half of the diagrams for scattering with rotation of the color state of dipoles

(25) allow a direct calculation of the jet–jet inclusive cross section in terms of the color dipole cross section $\sigma(\mathbf{r})$. But evaluation of the 6-fold Fourier transform is a nontrivial task.

We first note that the difference between Σ_2 and $\sigma_{11} = \sigma(\mathbf{r}) + \sigma(\mathbf{r}')$ is of the second or higher order in the off-diagonal σ_{18}, see Eq. (24). Consequently, the first two lines in Sylvester expansion (25) start with terms proportional to σ_{18}^2, whereas the last line starts with terms proportional to σ_{18}. It is then convenient to represent (25) as the impulse approximation (IA) term times the nuclear distortion factor $D_A(\mathbf{s}, \mathbf{r}, \mathbf{r}', \mathbf{b})$,

$$\sum_{A^*}\sum_{km}\langle 1; A|S_A^*(\mathbf{b}'_+, \mathbf{b}'_-)|A^*; c_{km}\rangle \times$$
$$\times \langle c_{km}; A^*|S_A(\mathbf{b}_+, \mathbf{b}_-)|A; 1\rangle -$$
$$- \langle 1; A|S_A^*(\mathbf{b}'_+, \mathbf{b}'_-)|A; 1\rangle\langle 1; A|S_A(\mathbf{b}_+, \mathbf{b}_-)|A; 1\rangle =$$
$$= T(\mathbf{b})\Sigma_{18}(\mathbf{s}, \mathbf{r}, \mathbf{r}')D_A(\mathbf{s}, \mathbf{r}, \mathbf{r}', \mathbf{b}), \quad (26)$$

whence

$$\frac{d\sigma_{in}}{d\mathbf{b}\, dz\, d\mathbf{p}_+ d\mathbf{p}_-} = \frac{1}{2(2\pi)^4} \times$$
$$\times \int d\mathbf{s}\, d\mathbf{r}\, d\mathbf{r}' \exp[-i(\mathbf{p}_+ + \mathbf{p}_-)\mathbf{s} + i\mathbf{p}_-(\mathbf{r}' - \mathbf{r})] \times$$
$$\times \Psi^*(Q^2, z, \mathbf{r}')\Psi(Q^2, z, \mathbf{r})T(\mathbf{b}) \times$$
$$\times \Sigma_{18}(\mathbf{s}, \mathbf{r}, \mathbf{r}')D_A(\mathbf{s}, \mathbf{r}, \mathbf{r}', \mathbf{b}). \quad (27)$$

As an introduction to nuclear $k_\perp$-factorization, we start with forward hard jets with the momenta $\mathbf{p}_\pm^2 \gtrsim Q_A^2$, which are produced from interactions with the target nucleus of small color dipoles in the incident photon such that diffractive nuclear attenuation effects can be neglected. We proceed with the formulation of the Fourier representations for each factor in (26). The application of integral representation (1) gives

$$\Sigma_{18}(\mathbf{s}, \mathbf{r}, \mathbf{r}') =$$
$$= [\sigma(\mathbf{s}) - \sigma(\mathbf{s} + \mathbf{r}') - \sigma(\mathbf{s} - \mathbf{r}) + \sigma(\mathbf{s} - \mathbf{r} + \mathbf{r}')] =$$
$$= \alpha_S\sigma_0 \int d\boldsymbol{\kappa} f(\boldsymbol{\kappa}) e^{i\boldsymbol{\kappa}\cdot\mathbf{s}} \left(1 - e^{i\boldsymbol{\kappa}\cdot\mathbf{r}'}\right) \times$$
$$\times \left(1 - e^{-i\boldsymbol{\kappa}\cdot\mathbf{r}}\right). \quad (28)$$

Hard jets correspond to $|\mathbf{r}|, |\mathbf{r}'| \ll |\mathbf{s}|$. Then the two eigenvalues are $\Sigma_2 \approx \sigma_{11}$ and $\Sigma_1 \approx \sigma_{88} \approx 2\lambda_c\sigma(\mathbf{s})$ with

$\lambda_c = N_c^2/(N_c^2-1) = C_A/2C_F$, where C_F and C_A are the Casimir operators for the fundamental and adjoint representations of $SU(N_c)$. Because $\Sigma_2 \approx \sigma_{11} \approx 0$, only the last term, proportional to σ_{18}, must be kept in Sylvester expansion (25), and the nuclear distortion factor takes the simple form

$$D_A(\mathbf{s},\mathbf{r},\mathbf{r}',\mathbf{b}) = \frac{2}{(\Sigma_2-\Sigma_1)T(\mathbf{b})} \times \times \left\{\exp\left[-\frac{1}{2}\Sigma_1 T(\mathbf{b})\right] - \exp\left[-\frac{1}{2}\Sigma_2 T(\mathbf{b})\right]\right\} = = \frac{1-\exp\left[-\frac{1}{2}\Sigma_1 T(\mathbf{b})\right]}{\frac{1}{2}\Sigma_1 T(\mathbf{b})}. \quad (29)$$

The Fourier representation for the nuclear distortion factor $D_A(\mathbf{s},\mathbf{r},\mathbf{r}')$ is readily obtained from the NSS representation [5, 6] for the nuclear attenuation factor,

$$\exp\left[-\frac{1}{2}\sigma(\mathbf{s})T(\mathbf{b})\right] = = \exp\left[-\nu_A(\mathbf{b})\right]\exp\left[\nu_A(\mathbf{b})\int d\boldsymbol{\kappa} f(\boldsymbol{\kappa})e^{i\boldsymbol{\kappa}\cdot\mathbf{s}}\right] = = \exp\left[-\nu_A(\mathbf{b})\right]\sum_{j=0}^{\infty}\frac{\nu_A^j(\mathbf{b})}{j!}\int d\boldsymbol{\kappa} f^{(j)}(\boldsymbol{\kappa})e^{i\boldsymbol{\kappa}\cdot\mathbf{s}} = = \int d\boldsymbol{\kappa}\Phi(\nu_A(\mathbf{b}),\boldsymbol{\kappa})e^{i\boldsymbol{\kappa}\cdot\mathbf{s}}, \quad (30)$$

in terms of the nuclear WW glue per unit area in the impact parameter plane, $\phi_{WW}(\nu_A(\mathbf{b}),\boldsymbol{\kappa})$, defined in [5],

$$\Phi(\nu_A(\mathbf{b}),\boldsymbol{\kappa}) = \sum_{j=0} w_j(\nu_A(\mathbf{b}))f^{(j)}(\boldsymbol{\kappa}) = = \exp[-\nu_A(\mathbf{b})]f^{(0)}(\boldsymbol{\kappa}) + \phi_{WW}(\nu_A(\mathbf{b}),\boldsymbol{\kappa}). \quad (31)$$

Here,

$$\nu_A(\mathbf{b}) = \frac{1}{2}\alpha_S(r)\sigma_0 T(\mathbf{b}) \quad (32)$$

and

$$w_j(\nu_A(\mathbf{b})) = \frac{\nu_A^j(\mathbf{b})}{j!}\exp\left[-\nu_A(\mathbf{b})\right] \quad (33)$$

is the probability of finding j spatially overlapping nucleons in a Lorentz-contracted nucleus, and

$$f^{(j)}(\boldsymbol{\kappa}) = \int\prod_{i=1}^{j} d\boldsymbol{\kappa}_i f(\boldsymbol{\kappa}_i)\delta(\boldsymbol{\kappa}-\sum_{i=1}^{j}\boldsymbol{\kappa}_i), \quad f^{(0)}(\boldsymbol{\kappa}) = \delta(\boldsymbol{\kappa}) \quad (34)$$

is a collective gluon field of j overlapping nucleons. As usual, the strong coupling in (32) must be taken at the hardest relevant scale [34].

The denominator Σ_1 in (29) is problematic from the point of view of the Fourier transform but can be eliminated by the integral representation,

$$D_A(\mathbf{s}) = \int_0^1 d\beta \exp\left[-\frac{1}{2}\beta\Sigma_1 T(\mathbf{b})\right] = = \int_0^1 d\beta\int d\boldsymbol{\kappa}\Phi(2\beta\lambda_c\nu_A(\mathbf{b}),\boldsymbol{\kappa})e^{i\boldsymbol{\kappa}\cdot\mathbf{s}}. \quad (35)$$

Here, β has the meaning of the fraction of the nuclear thickness that the $q\bar{q}$ pair propagates in the color octet state. The introduction of this distortion factor in (27) is straightforward and gives our central result for the hard jet–jet inclusive cross section:

$$\frac{d\sigma_{in}}{d\mathbf{b}dz\,d\mathbf{p}_+d\boldsymbol{\Delta}} = T(\mathbf{b})\int d\boldsymbol{\kappa} \times \times \int_0^1 d\beta\,\Phi(2\beta\lambda_c\nu_A(\mathbf{b}),\boldsymbol{\Delta}-\boldsymbol{\kappa})\frac{d\sigma_N}{dz\,d\mathbf{p}_+d\boldsymbol{\kappa}}. \quad (36)$$

Because $\mathbf{r}^2 \sim 1/\mathbf{p}_+^2$ for hard jets, we must use $\alpha_S(\mathbf{p}_+^2)$ in the evaluation of $\nu_A(\mathbf{b})$. For a thin nucleus with $\nu_A(\mathbf{b}) \ll 1$, we have $\Phi(2\beta\lambda_c\nu_A(\mathbf{b}),\boldsymbol{\Delta}-\boldsymbol{\kappa}) = \delta(\boldsymbol{\Delta}-\boldsymbol{\kappa})$, see Eq. (31), and recover the IA result

$$\frac{d\sigma_{in}}{d\mathbf{b}\,dz\,d\mathbf{p}_+d\boldsymbol{\Delta}} = T(\mathbf{b})\frac{d\sigma_N}{dz\,d\mathbf{p}_+d\boldsymbol{\Delta}}. \quad (37)$$

Our result (36) for nuclear broadening of the acoplanarity momentum distribution of hard dijets can be regarded as a nuclear counterpart of the $k_\perp$-factorization result (7) for a free nucleon target.

The probabilistic form of convolution (36) for the differential cross section on a free nucleon target with the manifestly positively defined distribution $\Phi(2\beta\lambda_c\nu_A(\mathbf{b}),\boldsymbol{\kappa})$ can be understood as follows. Hard jets originate from small color dipoles. Their interaction with gluons of the target nucleus is suppressed by the mutual neutralization of color charges of the quark and antiquark in the small-size color-singlet $q\bar{q}$ state, which is manifest from the small cross section for a free nucleon target, see Eq. (7). The first inelastic interaction inside the nucleus converts the $q\bar{q}$ pair into the color-octet state in which color charges of the quark and antiquark do not neutralize each other, rescatterings of the quark and antiquark in the collective color field of intranuclear nucleons become uncorrelated, and the broadening of the momentum distribution with nuclear thickness follows a probabilistic picture.

5. NONLINEAR NUCLEAR $k_\perp$-FACTORIZATION FOR BREAKUP OF PHOTONS INTO SEMIHARD DIJETS: LARGE-N_c APPROXIMATION

We can now relax the hardness restriction and consider semihard dijets, $|\mathbf{p}_\pm| \sim Q_A$. In this section, we give a consistent treatment of this case in the venerable large-N_c approximation. Our formulation can be called a nonlinear nuclear generalization of the $k_\perp$-factorization.

The crucial point is that in the large-N_c approximation, $\Sigma_2 = \sigma_{11} = \sigma(\mathbf{r}) + \sigma(\mathbf{r}')$, and therefore only the last term in Sylvester expansion (25) contributes to the jet–jet inclusive cross section. The nuclear distortion factor is still given by Eq. (29), but for finite Σ_2. Slightly generalizing (35) and using

$$\Sigma_1 = \sigma(\mathbf{s}) + \sigma(\mathbf{s} + \mathbf{r}' - \mathbf{r}), \tag{38}$$

we can recast the distortion factor in the form

$$\begin{aligned} D_A(\mathbf{s},\mathbf{r},\mathbf{r}',\mathbf{b}) &= \\ &= \int\limits_0^1 d\beta \exp\left\{-\frac{1}{2}[\beta\Sigma_1 + (1-\beta)\Sigma_2]T(\mathbf{b})\right\} = \\ &= \int\limits_0^1 d\beta \exp\left\{-\frac{1}{2}(1-\beta)[\sigma(\mathbf{r}) + \sigma(\mathbf{r}')]T(\mathbf{b})\right\} \times \\ &\quad \times \exp\left\{-\frac{1}{2}\beta[\sigma(\mathbf{s}) + \sigma(\mathbf{s}+\mathbf{r}'-\mathbf{r})]T(\mathbf{b})\right\}, \end{aligned} \tag{39}$$

where the different exponential factors admit a simple interpretation. The first and the second describe the intranuclear distortion of the incoming color-singlet $q\bar{q}$ and $q'\bar{q}'$ dipole state, whereas the last two factors describe the distortion of the outgoing color-octet $(q\bar{q})$ and $(q'\bar{q}')$ states. Application of the NSS representation [6] to the attenuation factors in (39) yields

$$\begin{aligned} D_A(\mathbf{s},\mathbf{r},\mathbf{r}',\mathbf{b}) &= \\ &= \int\limits_0^1 d\beta \int d\boldsymbol{\kappa}_1 \Phi((1-\beta)\nu_A(\mathbf{b}),\boldsymbol{\kappa}_1)\exp(-i\boldsymbol{\kappa}_1\cdot\mathbf{r}) \times \\ &\quad \times \int d\boldsymbol{\kappa}_2 \Phi((1-\beta)\nu_A(\mathbf{b}),\boldsymbol{\kappa}_2)\exp(i\boldsymbol{\kappa}_2\cdot\mathbf{r}) \times \\ &\quad \times \int d\boldsymbol{\kappa}_3 \Phi(\beta\nu_A(\mathbf{b}),\boldsymbol{\kappa}_3)\exp[i\boldsymbol{\kappa}_3\cdot(\mathbf{s}+\mathbf{r}'-\mathbf{r})] \times \\ &\quad \times \int d\boldsymbol{\kappa}_4 \Phi(\beta\nu_A(\mathbf{b}),\boldsymbol{\kappa}_4)\exp(i\boldsymbol{\kappa}_4\cdot\mathbf{r}). \end{aligned} \tag{40}$$

The integral representation in (39) furnishes two important tasks: it removes $\Sigma_1 - \Sigma_2$ from the denominator in (25) and gives the Fourier transform (40) of the nuclear distortion factor as a product of manifestly positive-definite nuclear WW gluon distributions. Finally, the jet–jet inclusive cross section takes the form

$$\begin{aligned} \frac{d\sigma_{in}}{d\mathbf{b}\,dz\,d\mathbf{p}_-d\boldsymbol{\Delta}} &= \frac{1}{2(2\pi)^2}\alpha_S\sigma_0 T(\mathbf{b}) \times \\ &\quad \times \int\limits_0^1 d\beta \int d\boldsymbol{\kappa}_1 d\boldsymbol{\kappa}_2 d\boldsymbol{\kappa}_3 d\boldsymbol{\kappa} f(\boldsymbol{\kappa}) \times \\ &\quad \times \Phi(\beta\nu_A(\mathbf{b}),\boldsymbol{\Delta}-\boldsymbol{\kappa}_3-\boldsymbol{\kappa})\Phi(\beta\nu_A(\mathbf{b}),\boldsymbol{\kappa}_3) \times \\ &\quad \times \Phi((1-\beta)\nu_A(\mathbf{b}),\boldsymbol{\kappa}_1)\Phi((1-\beta)\nu_A(\mathbf{b}),\boldsymbol{\kappa}_2) \times \\ &\quad \times \{\langle\gamma^*|z,\mathbf{p}_-+\boldsymbol{\kappa}_2+\boldsymbol{\kappa}_3\rangle - \langle\gamma^*|z,\mathbf{p}_-+\boldsymbol{\kappa}_2+\boldsymbol{\kappa}_3+\boldsymbol{\kappa}\rangle\} \times \\ &\quad \times \{\langle z,\mathbf{p}_-+\boldsymbol{\kappa}_1+\boldsymbol{\kappa}_3|\gamma^*\rangle - \langle z,\mathbf{p}_-+\boldsymbol{\kappa}_1+\boldsymbol{\kappa}_3+\boldsymbol{\kappa}|\gamma^*\rangle\} = \\ &= \frac{1}{2(2\pi)^2}\alpha_S\sigma_0 T(\mathbf{b}) \int\limits_0^1 d\beta \int d\boldsymbol{\kappa}_3 d\boldsymbol{\kappa} f(\boldsymbol{\kappa}) \times \\ &\quad \times \Phi(\beta\nu_A(\mathbf{b}),\boldsymbol{\Delta}-\boldsymbol{\kappa}_3-\boldsymbol{\kappa})\Phi(\beta\nu_A(\mathbf{b}),\boldsymbol{\kappa}_3) \times \\ &\quad \times \left| \int d\boldsymbol{\kappa}_1 \Phi((1-\beta)\nu_A(\mathbf{b}),\boldsymbol{\kappa}_1) \times \right. \\ &\quad \times \{\langle\gamma^*|z,\mathbf{p}_- + \boldsymbol{\kappa}_1 + \boldsymbol{\kappa}_3\rangle - \\ &\quad \left. - \langle\gamma^*|z,\mathbf{p}_- + \boldsymbol{\kappa}_1 + \boldsymbol{\kappa}_3 + \boldsymbol{\kappa}\rangle\}\right|^2. \end{aligned} \tag{41}$$

This is our central result for the inclusive cross section of the photon breakup into dijets on nuclei. It demonstrates how the broadening of the transverse momentum distribution of dijets is uniquely calculable in terms of the collective WW glue of a nucleus and as such must be regarded as a nonlinear $k_\perp$-factorization for the inclusive dijet cross section.

The last form of (41) shows clearly that the integrand is manifestly positive-valued. Returning to (39) and (40), we can identify the convolution of the collective nuclear WW glue $\Phi((1-\beta)\nu_A(\mathbf{b}),\boldsymbol{\kappa}_1)$ with the photon wave functions in the last form in (41) as an effect of distortions of the photon wave function when the $q\bar{q}$ pair propagates in the state that is still color-singlet.

We finally consider the limiting case where $|\mathbf{p}_-|, |\boldsymbol{\Delta}| \lesssim Q_A$. In our analysis [5] of the single particle spectrum, we discovered that the transverse momentum distribution of sea quarks is dominated by anticollinear, anti-DGLAP splitting of gluons into sea when the transverse momentum of the parent gluons is larger than the momentum of sea quarks. As stated in the Introduction, this strongly suggests a complete azimuthal decorrelation of forward minijets with the transverse momenta below the saturation scale, $p_\pm \lesssim Q_A$. Our analysis of $f^{(j)}(\boldsymbol{\kappa})$ in Appendix C shows that for the average DIS on realistic nuclei,

Q_A^2 does not exceed several $(\mathrm{GeV}/c)^2$, and hence this regime is a somewhat academic one (see Sec. 6, however). We nevertheless assume that Q_A is so large that jets with $p_\pm \lesssim Q_A$ are measurable.

We note that $|\boldsymbol{\kappa}_i| \sim Q_A$, and we can therefore neglect $\mathbf{p}_-$ in the photon wave functions and the decorrelation momentum $\boldsymbol{\Delta}$ in the argument of $\Phi(\beta\nu_A(\mathbf{b}), \boldsymbol{\Delta} - \boldsymbol{\kappa}_3 - \boldsymbol{\kappa})$. The approximation

$$\left| \int d\boldsymbol{\kappa}_1 \Phi((1-\beta)\nu_A(\mathbf{b}), \boldsymbol{\kappa}_1) \{\langle\gamma^*|z, \mathbf{p}_- + \boldsymbol{\kappa}_1 + \boldsymbol{\kappa}_3\rangle - \right.$$
$$\left. - \langle\gamma^*|z, \mathbf{p}_- + \boldsymbol{\kappa}_1 + \boldsymbol{\kappa}_3 + \boldsymbol{\kappa}\rangle\} \right|^2 \approx$$
$$\approx \left| \langle\gamma^*|z, \boldsymbol{\kappa}_3\rangle - \langle\gamma^*|z, \boldsymbol{\kappa}_3 + \boldsymbol{\kappa}\rangle \right|^2 \quad (42)$$

is then justified in (41). The principal point is that the minijet–minijet inclusive cross section is independent of either the minijet or the decorrelation momentum, which proves the disappearance of the azimuthal decorrelation of minijets with the transverse momentum below the saturation scale.

6. AZIMUTHAL DECORRELATION OF DIJETS IN DIS OFF NUCLEI: NUMERICAL ESTIMATES

The azimuthal decorrelation of two jets is quantified by the mean transverse acoplanarity momentum squared $\langle \boldsymbol{\Delta}_\perp^2(\mathbf{b})\rangle$, where $\boldsymbol{\Delta}_\perp$ is transverse to the axis of the jet with the higher momentum (Fig. 3). Here, we present numerical estimates for hard dijets,

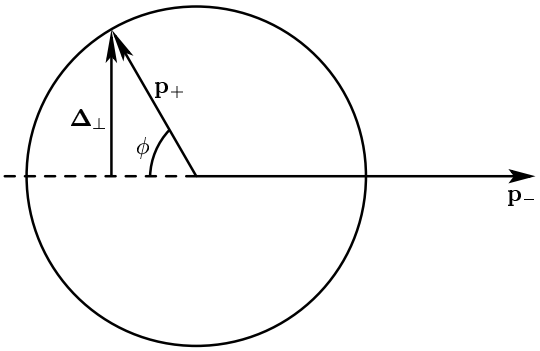

Fig. 3. The definition of the dijet configurations considered and of the transverse component of the acoplanarity momentum $\boldsymbol{\Delta}_\perp$

$|\mathbf{p}_+| \gg Q_A$. The convolution property of hard dijet cross section (35) suggests that

$$\langle \boldsymbol{\Delta}_\perp^2(\mathbf{b})\rangle_A = \left\{ \int\limits_{\mathcal{C}} d\mathbf{p}_-\, \boldsymbol{\Delta}_\perp^2 \frac{d\sigma_N}{dz\, d\mathbf{p}_+ d\mathbf{p}_-} \right\} \times$$
$$\times \left\{ \int\limits_{\mathcal{C}} d\mathbf{p}_- \frac{d\sigma_N}{dz\, d\mathbf{p}_+ d\mathbf{p}_-} \right\}^{-1} \approx$$
$$\approx \langle \boldsymbol{\kappa}_\perp^2(\mathbf{b})\rangle_A + \langle \boldsymbol{\Delta}_\perp^2\rangle_N, \quad (43)$$

where $\langle \boldsymbol{\Delta}_\perp^2\rangle_N$ refers to DIS on a free nucleon and $\langle \boldsymbol{\kappa}_\perp^2(\mathbf{b})\rangle_A$ is the nuclear broadening term:

$$\langle \boldsymbol{\kappa}_\perp^2(\mathbf{b})\rangle_A = \left\{ \int\limits_{\mathcal{C}} d\boldsymbol{\kappa}\, \boldsymbol{\kappa}_\perp^2\, \Phi(2\beta\lambda_c\nu_A(\mathbf{b}), \boldsymbol{\kappa}) \right\} \times$$
$$\times \left\{ \int\limits_{\mathcal{C}} d\boldsymbol{\kappa}\, \Phi(2\beta\lambda_c\nu_A(\mathbf{b}), \boldsymbol{\kappa}) \right\}^{-1}. \quad (44)$$

The sign «$\approx$» in (43) reflects the kinematical limitations $\mathcal{C}$ on $\mathbf{p}_-$ and $\boldsymbol{\kappa}$ in the practical evaluation of the acoplanarity distribution. In a typical final state shown in Fig. 3, it is the harder jet with the larger transverse momentum that defines the jet axis, and the acoplanarity momentum $\boldsymbol{\Delta}$ is defined in terms of components of the momentum of the softer jet with respect to that axis, see, e.g., [20]. For definiteness, we present numerical estimates for the Gedanken experiment in which we classify an event as a dijet if the quark and antiquark are produced in different hemispheres, i.e., if the azimuthal angle $\pi - \phi$ between the two jets is below $\pi/2$, the quark jet has fixed $|\mathbf{p}_+|$, and the antiquark jet has a higher transverse momentum, $|\mathbf{p}_+| \lesssim |\mathbf{p}_-| \lesssim 10|\mathbf{p}_+|$ (in the discussion of the experimental data, one often refers to the higher momentum jet as the trigger jet and the softer jet as the away jet [20]).

The free-nucleon quantity $\langle \boldsymbol{\Delta}_\perp^2\rangle_N$ is evaluated from Eq. (43) with free nucleon cross section (7). For evaluation purposes, we can start with the small-$\boldsymbol{\Delta}$ expansion for excitation of hard $(\mathbf{p}_+^2 \gg \varepsilon^2 = z(1-z)Q^2)$, light flavor dijets from transverse photons,

$$\frac{d\sigma_N}{dz\, d\mathbf{p}_+ d\boldsymbol{\Delta}} \approx \frac{1}{\pi} e_f^2 \alpha_{em} \alpha_S(\mathbf{p}_+^2) \left[z^2 + (1-z)^2\right] \times$$
$$\times \frac{1}{\Delta^4} \frac{\partial G(x, \boldsymbol{\Delta}^2)}{\partial \ln(\boldsymbol{\Delta}^2)} \frac{\boldsymbol{\Delta}^2}{(\varepsilon^2 + \mathbf{p}_+^2)(\varepsilon^2 + \mathbf{p}_+^2 + \boldsymbol{\Delta}^2)}. \quad (45)$$

The form of the last factor in (45) only mimics its le-

veling off at $\mathbf{\Delta}^2 \gtrsim \mathbf{p}_+^2$, see Eq. (7). In the denominator of (43), we then find the typical logarithmic integral

$$\frac{1}{\pi}\int\limits_0^\pi d\phi \int^{\mathbf{p}_+^2} \frac{d\mathbf{\Delta}^2}{\mathbf{\Delta}^2}\,\frac{\partial G(x,\mathbf{\Delta}^2)}{\partial \ln \mathbf{\Delta}^2} = G(x,\mathbf{p}_+^2), \qquad (46)$$

to be compared with the numerator of the form

$$\frac{1}{\pi}\int\limits_0^\pi d\phi \sin^2\phi \int^{\mathbf{p}_+^2} d\mathbf{\Delta}^2\,\frac{\partial G(x,\mathbf{\Delta}^2)}{\partial \ln \mathbf{\Delta}^2} \sim \sim \frac{1}{2}\mathbf{p}_+^2\,\mathcal{F}(x,\mathbf{p}_+^2). \qquad (47)$$

More accurate numerical estimates for the selection criteria of our Gedanken experiment suggest the numerical factor ≈ 0.7 in (47); the expression

$$\langle \mathbf{\Delta}_\perp^2\rangle_N = \left\{\int\limits_{p_+} d\mathbf{p}_-\,\mathbf{\Delta}_\perp^2\,\frac{d\sigma_N}{dz\,d\mathbf{p}_+ d\mathbf{p}_-}\right\}\times \times\left\{\int\limits_{p_+} d\mathbf{p}_-\,\frac{d\sigma_N}{dz\,d\mathbf{p}_+ d\mathbf{p}_-}\right\}^{-1} \approx \approx 0.7\frac{\mathcal{F}(x,\mathbf{p}_+^2)}{G(x,\mathbf{p}_+^2)}\mathbf{p}_+^2 \qquad (48)$$

correctly describes the numerical results shown in Fig. 4. As far as the dijets are hard, $\mathbf{p}_+^2 \gtrsim z(1-z)Q^2 \sim \sim \frac{1}{4}Q^2$, the acoplanarity momentum distribution is independent of Q^2, which holds even better if we consider $\sigma_T + \sigma_L$. This point is illustrated in Fig. 4, where we show $\langle \mathbf{\Delta}_\perp^2\rangle_N$ at $z = 1/2$ for several values of Q^2. Because of this weak dependence on Q^2, we make no distinction between DIS and real photoproduction, $Q^2 = 0$, in what follows.

In practical evaluations of the nuclear contribution $\langle \boldsymbol{\kappa}_\perp^2(\mathbf{b})\rangle_A$, we can use the explicit expansion

$$\int\limits_0^1 d\beta\Phi(2\beta\lambda_c\nu_A(\mathbf{b}),\boldsymbol{\kappa}) = \sum_{j=0}^\infty w_A(\mathbf{b},j)f^{(j)}(\boldsymbol{\kappa}) = = \sum_{j=0}^\infty \frac{1}{j!}\,\frac{\gamma(j+1,2\lambda_c\nu_A(\mathbf{b}))}{2\lambda_c\nu_A(\mathbf{b})}f^{(j)}(\boldsymbol{\kappa}), \qquad (49)$$

where

$$\gamma(j,x) = \int\limits_0^x dy y^{j-1}e^{-y}$$

is the incomplete gamma-function. The properties of the collective glue for j overlapping nucleons, $f^{(j)}(\boldsymbol{\kappa})$, are presented in Appendix C. For a heavy nucleus, Eq. (49) can be approximated by its integrand at $\beta \approx 1/2$, i.e., by $\Phi(\lambda_c\nu_A(\mathbf{b}),\boldsymbol{\kappa})$. A slightly more accurate evaluation of the numerically important no-broadening contribution from $j = 0$ gives

$$\int\limits_0^1 d\beta\Phi(2\beta\lambda_c\nu_A(\mathbf{b}),\boldsymbol{\kappa}) \approx w_A(\mathbf{b},0)\delta(\boldsymbol{\kappa}) + + (1-w_A(\mathbf{b},0))\frac{1}{\pi}\,\frac{\lambda_c Q_A^2(\mathbf{b})}{(\boldsymbol{\kappa}^2+\lambda_c Q_A^2(\mathbf{b}))^2}, \qquad (50)$$

where Q_A^2 is given by Eq. (108) and

$$w_A(\mathbf{b},0) = \frac{1-\exp[-\nu_A(\mathbf{b})]}{\nu_A(\mathbf{b})} \qquad (51)$$

is the probability of the no-broadening contribution, which is still substantial for realistic nuclei. In our Gedanken experiment, $\langle \boldsymbol{\kappa}_\perp^2(\mathbf{b})\rangle_A$ must be evaluated over the constrained phase space $\mathcal{C}$, $\kappa_\perp \le |\mathbf{p}_+|$ and $\kappa_L > 0$, and analytic parameterization (50) gives

$$\langle \boldsymbol{\kappa}_\perp^2(\mathbf{b})\rangle_A \approx \lambda_c Q_A^2(\mathbf{b})\times \times\left[\ln\mathrm{tg}\left(\frac{\pi}{4}+\frac{1}{2}\,\mathrm{arctg}\,\frac{p_+}{\sqrt{\lambda_c}Q_A(\mathbf{b})}\right) - - \frac{p_+}{\sqrt{\lambda_c Q_A^2(\mathbf{b})+p_+^2}}\right]\times \times\frac{(1-w_A(\mathbf{b},0))\sqrt{\lambda_c Q_A^2(\mathbf{b})+p_+^2}}{w_A(\mathbf{b},0)\sqrt{\lambda_c Q_A^2(\mathbf{b})+p_+^2}+(1-w_A(\mathbf{b},0))p_+}. \qquad (52)$$

We recall that (43) and (52) must only be used for $|\mathbf{p}_+| \gg Q_A(\mathbf{b})$.

For the average DIS off heavy nuclei, the reference value is $\langle Q_{Au}^2(\mathbf{b})\rangle = 0.9\ (\mathrm{GeV}/c)^2$, see Appendix C. The atomic mass number dependence of the nuclear broadening $\langle \boldsymbol{\kappa}_\perp^2\rangle_A$ for jets with $p_+ = 4$ GeV/c in the average DIS off nucleus is shown in Fig. 5. The principal reason why $\langle \boldsymbol{\kappa}_\perp^2\rangle_A$ is numerically small compared to $\langle Q_{\mathrm{Au}}^2(\mathbf{b})\rangle$ is that even for such a heavy nucleus as ^{197}Au, the no-broadening probability in the average DIS is large, $\langle w_{\mathrm{Au}}(\mathbf{b},0)\rangle \approx 0.5$. Comparison of the free nucleon broadening $\langle \mathbf{\Delta}_\perp^2\rangle_N$ in Fig. 4 with the nuclear contribution $\langle \boldsymbol{\kappa}_\perp^2(\mathbf{b})\rangle_A$ in Fig. 5 shows that the nuclear mass number dependence of the azimuthal decorrelation of dijets in the average DIS off nuclei is relatively weak.

However, nuclear broadening is substantially stronger for a subsample of central DIS events at

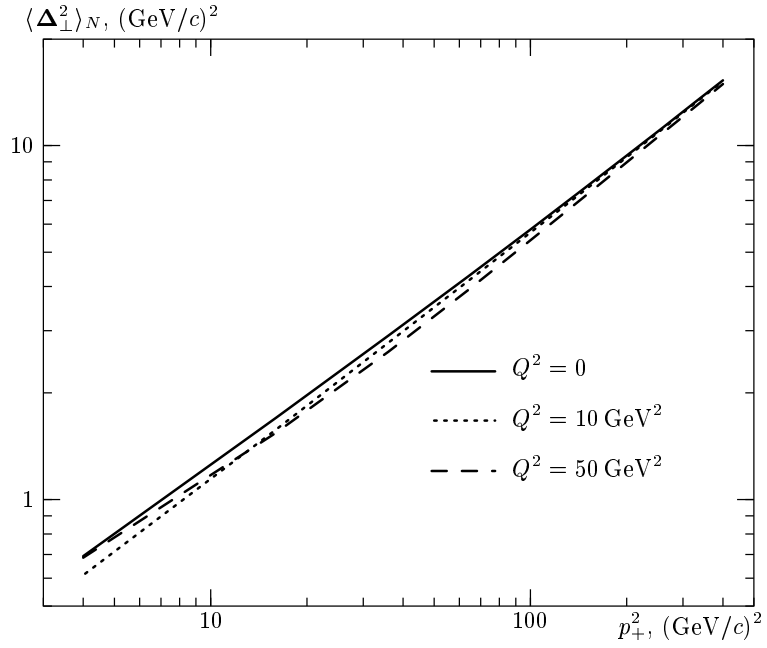

Fig. 4. The mean acoplanarity momentum squared $\langle \boldsymbol{\Delta}_\perp^2 \rangle_N$ for DIS off a free nucleon target with production of trigger jets with the transverse momentum higher than $\mathbf{p}_+$ for several values of Q^2. The numerical results are for $x = 0.01$ and the input unintegrated gluon structure of the proton is taken from Ref. [19]

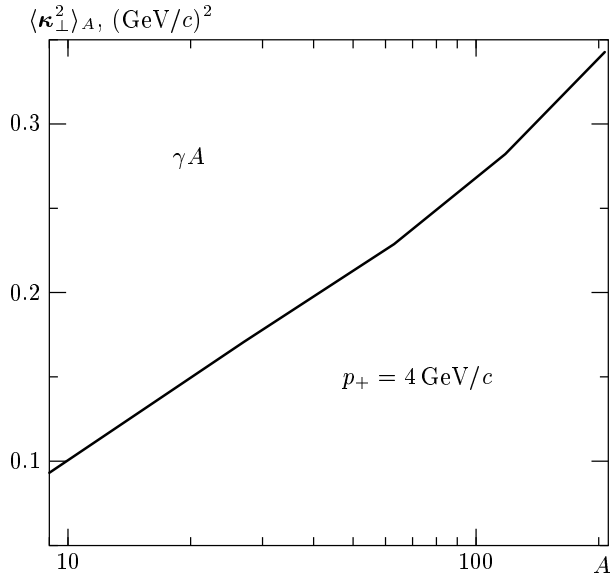

Fig. 5. The atomic mass number dependence of nuclear broadening contribution, $\langle \boldsymbol{\kappa}_\perp^2(\mathbf{b}) \rangle_A$, to the mean acoplanarity momentum squared for real photoproduction off nuclei at $x = 0.01$. The input unintegrated gluon SF of the proton is taken from Ref. [19]

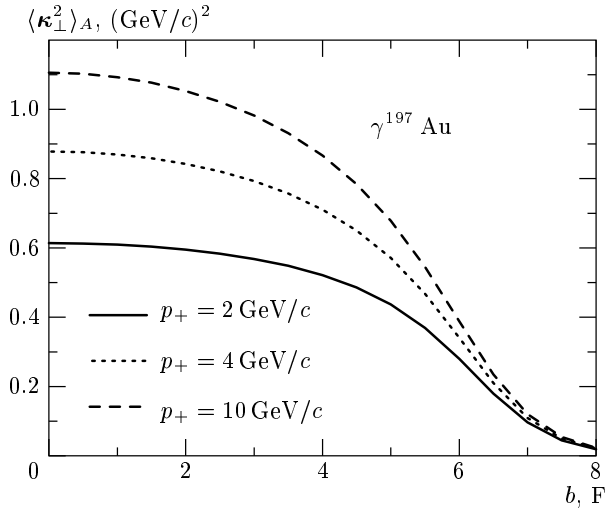

Fig. 6. The impact parameter dependence of the nuclear broadening contribution, $\langle \boldsymbol{\kappa}_\perp^2(\mathbf{b}) \rangle_A$, to the mean acoplanarity momentum squared from peripheral DIS at a large impact parameter to the central DIS at $\mathbf{b} = 0$ for several values of the away jet momentum p_+. The numerical results are for $x = 0.01$ and the input unintegrated gluon SF of the proton is taken from Ref. [19]

$\mathbf{b} \sim 0$. In Fig. 6, we show the dependence of the β-averaged nuclear broadening $\langle \boldsymbol{\kappa}_\perp^2(\mathbf{b}) \rangle_A$ on the impact parameter at several values of p_+ for the gold, ^{197}Au, target. There are two related sources

of the p_+ dependence of $\langle \boldsymbol{\kappa}_\perp^2(\mathbf{b})\rangle_A$. First, because $r, r' \sim 1/p_+$ for hard dijets, the strong coupling enters Eqs. (33) and (108) as $\alpha_S(\mathbf{p}_+^2)$. Then for hard jets, $\nu_A(\mathbf{b}) \propto \alpha_S(\mathbf{p}_+^2)$ and $w_A(\mathbf{b}=0,0)$ rises substantially with p_+ in the region of p_+ of practical interest, $1 \lesssim p_+ \lesssim 5$–$10$ GeV/c, where the strong coupling varies rapidly. For a nucleus with the mass number $A = 200$, it rises from $w_A(\mathbf{b}=0,0) \approx 0.12$ at $p_+ = 2$ GeV/c to ≈ 0.20 at 4 GeV/c, and to ≈ 0.25 at $p_+ = 10$ GeV/c (see [39] for the nuclear density parameterization). Second, for the same reason that $\nu_A(\mathbf{b}) \propto \alpha_S(\mathbf{p}_+^2)$, the contribution from large j in (49), and hence $Q_A^2(\mathbf{b})$, diminishes gradually with rising p_+, proportionally to $\alpha_S(\mathbf{p}_+^2)/\alpha_S(Q_A^2)$. In the region $p_+ \lesssim 10$ GeV/c of practical interest, we find that $\langle \boldsymbol{\kappa}_\perp^2(\mathbf{b})\rangle_A \sim Q_A^2(\mathbf{b})$.

We now compare the numerical results in Figs. 5 and 6 for $p_+ = 4$ GeV/c and the ^{197}Au target. According to Eq. (109) in Appendix C,

$$Q_A^2(0) = \left(\frac{4}{3} - 2\right) \langle Q_A^2(\mathbf{b})\rangle. \tag{53}$$

The no-broadening probability $w_A(\mathbf{b}=0,0) \approx 0.20$ for central DIS is substantially smaller than $\langle w_{Au}(\mathbf{b},0)\rangle \approx 0.5$ for average DIS. In conjunction with (53), this entails an enhancement of $\langle \boldsymbol{\kappa}_\perp^2(\mathbf{b})\rangle_A$ by the factor 2.5–3 from the average to central DIS. The same point is illustrated by the expectation value of j in (49) for the Au target: for jets with $p_+ = 4$ GeV/c, it decreases by the factor about 3 from $\langle j(\mathbf{b}=0)\rangle = 2.86$ to $\langle j\rangle_A = 0.87$ from the central to average DIS.

One can enhance Q_A^2 and the nuclear contribution $\langle \boldsymbol{\kappa}_\perp^2(\mathbf{b})\rangle_A$ even further by selecting the DIS events where the photon breaks up into a $q\bar{q}$ pair on the front face of the nucleus, which in the language of (36) corresponds to the contribution from $\beta \to 1$, see the discussion of (49). Experimentally, precisely such events are isolated by selecting very large multiplicities or very high transverse energies of the secondary particles produced (see [20] and references therein). Equation (36) then shows (also see the discussion of the $\beta \approx 1/2$ approximation in (49)) that for a very high multiplicity central DIS off the Au nucleus, $Q_A^2 \approx 2.5$ GeV^2 is quite feasible. Equation (52) shows that for such a large $Q_A^2 \approx 2.5$ GeV^2 and $p_+ = 5$–10 GeV/c of practical interest, $\langle \boldsymbol{\kappa}_\perp^2(\mathbf{b}=0)\rangle$ grows slower than proportionally to Q_A^2, and therefore the value of $\langle \boldsymbol{\kappa}_\perp^2(\mathbf{b}=0)\rangle$ for a high-multiplicity central DIS off Au nucleus is enhanced by the factor 4–5 from $\langle \boldsymbol{\kappa}_\perp^2\rangle_{\rm Au}$ for the average DIS.

We have an overall good understanding of gross features of nuclear azimuthal decorrelations in DIS off nuclei. We now comment on the recent finding by the STAR collaboration of the disappearance of a back-to-back high-$p_\perp$ hadron correlation occurring in passing from peripheral to central gold–gold collisions at RHIC [20]. Our experience with application of the color dipole formalism to hard hadron–nucleus interactions [17] suggests that our analysis of acoplanarity of forward hard jets can be generalized to mid-rapidity jets. This only requires choosing an appropriate system of dipoles, for instance, the open heavy flavor production can be treated in terms of the intranuclear propagation of the gluon–quark–antiquark system in the overall color-singlet state. At RHIC energies, jets with moderately large $p_\perp$ are mostly due to gluon–gluon collisions. In our language, this can be treated as a breakup of gluons into dijets, and azimuthal decorrelation of hard jets must be discussed in terms of intranuclear propagation of color-octet gluon–gluon dipoles. For such gluon–gluon dipoles, the relevant saturation scale Q_{8A}^2 is larger than that for the quark–antiquark dipoles by the factor $2\lambda_c = C_A/C_F = 9/4$ [24]. Arguably, distortions in the target and projectile nuclei add up in central nucleus–nucleus collisions and the effective thickness of nuclear matter is about twice that in DIS. The results shown in Fig. 5 then suggest that for central gold–gold collisions, the nuclear broadening of gluon–gluon dijets could be quite substantial, $\langle \boldsymbol{\kappa}_\perp^2(\mathbf{b}=0)\rangle_{\rm AuAu} \sim 3$–$4$ (GeV/c)^2 for the average central Au–Au collisions and even twice larger if collisions occur at the front surface of the colliding nuclei.

The principal effect of nuclear broadening is a reduction of the probability of observing back-to-back jets,

$$P(b) \propto \frac{\langle \boldsymbol{\Delta}_\perp^2\rangle_N}{\langle \boldsymbol{\kappa}_\perp^2(\mathbf{b})\rangle_A + \langle \boldsymbol{\Delta}_\perp^2\rangle_N}, \tag{54}$$

where $\langle \boldsymbol{\Delta}_\perp^2\rangle_N$ is to be compared to $\langle \boldsymbol{\kappa}_\perp^2(\mathbf{b})\rangle_A$. Equation (48) for the free nucleon case also holds for the gluon–gluon collisions. The results shown in Fig. 3 then entail that $\langle \boldsymbol{\Delta}_\perp^2\rangle_N \approx \langle \boldsymbol{\kappa}_\perp^2(0)\rangle_{\rm AuAu} \sim 3$–$4$ (GeV/c)^2 at the jet momentum $p_+ = p_J = 6$–8 GeV/c and our nuclear broadening becomes substantial for all jets with p_+ below the decorrelation threshold momentum p_J. In practice, the STAR collaboration studied the azimuthal correlation of two high-$p_\perp$ hadrons; for a quantitative correspondence between the STAR observable and the azimuthal decorrelation in the parent dijet, one must model the fragmentation of jets into hadrons (see [35] for the modern fragmentation schemes). We note here that the cutoff p_+ in our Gedanken experiment is related to the momentum cutoff $p_{T,min}$ of the associated tracks from the away jet, whereas our jet of the momen-

tum $\mathbf{p}_-$ can be regarded as a counterpart of the trigger jet of STAR. The STAR cutoff $p_T = 2$ GeV/c corresponds to parent jets with the transverse momentum $p_+ \sim (2\text{–}3)p_T = 4\text{–}6$ GeV/c, which is comparable to, or even smaller than the decorrelation threshold momentum $p_J = 6\text{–}8$ GeV/c. Equation (54) then suggests that in the kinematics of STAR, the probability to observe the back-to-back away and trigger jets approximately reduces to half, and perhaps even stronger, from peripheral to central Au–Au collisions, and our azimuthal decorrelation may therefore substantially contribute to the STAR effect.

In practical consideration of azimuthal decorrelations in central heavy ion collisions, the above distortions of the produced jet–jet inclusive spectrum due to interactions with the nucleons of the target and projectile ions must be complemented by rescatterings of the parent high-$p_\perp$ partons on the abundantly produced secondary hadrons. Our nuclear decorrelation effect must be dominant and reinteractions with secondary particles must be marginal in pA collisions, where we expect $\langle \boldsymbol{\kappa}_\perp^2(0)\rangle_{p\mathrm{Au}} \approx 1.5$ (GeV/c)^2 for central collisions and even $\langle \boldsymbol{\kappa}_\perp^2(0)\rangle_{p\mathrm{Au}} \approx 3$ (GeV/c)^2 is feasible for central collisions in the regime of $\beta \to 1$, i.e., with the limiting high multiplicity.

7. NUCLEAR $k_\perp$-FACTORIZATION FOR $1/N_c^2$ CORRECTIONS TO THE PHOTON BREAKUP

Having established nuclear $k_\perp$-factorization properties of the dijet cross section to the leading order of the large-N_c approximation, we turn to the $1/N_c^2$-corrections and demonstrate that with one simple exception, the $1/N_c^2$-expansion can be regarded as the higher-twist expansion. The two sources of the $1/N_c^2$-corrections to the nuclear distortion factor are higher-order terms in the off-diagonal σ_{18} matrix element and the terms proportional to $1/(N_c^2-1)$ in σ_{88}, Eq. (21). We note that σ_{88} can be decomposed as

$$\sigma_{88} = \sigma(\mathbf{s}) + \sigma(\mathbf{s}-\mathbf{r}+\mathbf{r}') + \frac{2\Sigma_{18}(\mathbf{s},\mathbf{r},\mathbf{r}')}{N_c^2-1} + \\ + \frac{\sigma(\mathbf{s}) + \sigma(\mathbf{s}-\mathbf{r}+\mathbf{r}') - \sigma(\mathbf{r}) - \sigma(\mathbf{r}')}{N_c^2-1} = \\ = \frac{N_c^2}{N_c^2-1}[\sigma(\mathbf{s}) + \sigma(\mathbf{s}-\mathbf{r}+\mathbf{r}')] + \frac{2\Sigma_{18}(\mathbf{s},\mathbf{r},\mathbf{r}')}{N_c^2-1} - \\ - \frac{\Delta\Sigma_{88}(\mathbf{r},\mathbf{r}')}{N_c^2-1}, \quad (55)$$

where

$$\Delta\Sigma_{88}(\mathbf{r},\mathbf{r}') = \sigma(\mathbf{r}) + \sigma(\mathbf{r}') \quad (56)$$

and we exactly reabsorbed one part of the $1/N_c^2$-correction into the leading large-N_c term of σ_{88} by scaling it with the color factor λ_c.

After some algebra, we find

$$\langle 11|S_{4A}(\mathbf{b}'_+,\mathbf{b}'_-,\mathbf{b}_+,\mathbf{b}_-)|11\rangle = \\ = \exp\left\{-\frac{1}{2}[\sigma(\mathbf{r})+\sigma(\mathbf{r}')]T(\mathbf{b})\right\} + \\ + \frac{\Sigma_{18}^2(\mathbf{s},\mathbf{r},\mathbf{r}')T^2(\mathbf{b})}{4(N_c^2-1)}\int\limits_0^1 d\beta \int\limits_0^\beta d\beta_1 \times \\ \times \exp\left\{-\frac{1}{2}(1-\beta+\beta_1)[\sigma(\mathbf{r})+\sigma(\mathbf{r}')]T(\mathbf{b})\right\} \times \\ \times \exp\left\{-\frac{1}{2}(\beta-\beta_1)[\sigma(\mathbf{s})+\sigma(\mathbf{s}-\mathbf{r}+\mathbf{r}')]T(\mathbf{b})\right\}. \quad (57)$$

The first term in (57) is canceled by the subtraction of coherent diffractive term (22) in (8) and (25), and therefore only the subleading term in (57), proportional to $1/(N_c^2-1)$, contributes to the dijet cross section. Evaluation of corrections to the leading term of the Sylvester expansion is somewhat more complicated,

$$\sqrt{N_c^2-1}\langle 88|S_{4A}(\mathbf{b}'_+,\mathbf{b}'_-,\mathbf{b}_+,\mathbf{b}_-)|11\rangle = \\ = \frac{1}{2}\Sigma_{18}(\mathbf{s},\mathbf{r},\mathbf{r}')T(\mathbf{b}) \times \\ \times \left[\int\limits_0^1 d\beta \exp\left\{-\frac{1}{2}\beta[\sigma(\mathbf{r})+\sigma(\mathbf{r}')]T(\mathbf{b})\right\} \times \right. \\ \times \exp\left\{-\frac{1}{2}(1-\beta)\sigma_{88}T(\mathbf{b})\right\} + \\ + \frac{\Sigma_{18}^2(\mathbf{s},\mathbf{r},\mathbf{r}')T^2(\mathbf{b})}{4(N_c^2-1)}\int\limits_0^1 d\beta\int\limits_0^\beta d\beta_1\int\limits_0^{\beta_1} d\beta_2 \times \\ \times \exp\left\{-\frac{1}{2}(\beta-\beta_1+\beta_2)[\sigma(\mathbf{r})+\sigma(\mathbf{r}')]T(\mathbf{b})\right\} \times \\ \times \exp\left\{-\frac{1}{2}(1-\beta+\beta_1-\beta_2) \times \right. \\ \left.\left. \times [\sigma(\mathbf{s})+\sigma(\mathbf{s}-\mathbf{r}+\mathbf{r}')]T(\mathbf{b})\right\}\right]. \quad (58)$$

The first term in (58) contains the attenuation factor, where σ_{88} is still the exact diagonal matrix element, and we must isolate the leading term and the $1/(N_c^2-1)$-correction,

$$\exp\left\{-\frac{1}{2}(1-\beta)\sigma_{88}T(\mathbf{b})\right\} =$$
$$= \exp\left\{-\frac{1}{2}(1-\beta)\lambda_c[\sigma(\mathbf{s})+\sigma(\mathbf{s}-\mathbf{r}+\mathbf{r}')]T(\mathbf{b})\right\}\times$$
$$\times\left\{1-\frac{(1-\beta)\Sigma_{18}(\mathbf{s},\mathbf{r},\mathbf{r}')T(\mathbf{b})}{N_c^2-1}+\right.$$
$$\left.+\frac{(1-\beta)\Delta\Sigma_{88}(\mathbf{r},\mathbf{r}')T(\mathbf{b})}{2(N_c^2-1)}\right\}. \quad (59)$$

The fundamental reason why the different components of the second term, proportional to $1/(N_c^2-1)$, in Eq. (21) are treated differently is that the NSS representation [6] with a positive-valued Fourier transform holds only for attenuating exponentials of the dipole cross section. The related expansion for the rising exponential $\exp[\frac{1}{2}\sigma(\mathbf{r})T(\mathbf{b})]$ can easily be written, but its Fourier transform is a sign-oscillating expansion,

$$\exp\left[\frac{1}{2}\sigma(\mathbf{s})T(\mathbf{b})\right] =$$
$$= \exp\left[2\nu_A(\mathbf{b})\right]\sum_{j=0}^{\infty}(-1)^j w_j(\nu_A(\mathbf{b}))\times$$
$$\times\int d\boldsymbol{\kappa} f^{(j)}(\boldsymbol{\kappa})\exp(i\boldsymbol{\kappa}\cdot\mathbf{s}). \quad (60)$$

Therefore, combining the two exponentials with similar exponents proportional to $[\sigma(\mathbf{r})+\sigma(\mathbf{r}')]$ in the first term of (57) is not guaranteed, because the sign of the exponent changes from attenuation to growth in the course of the β integration,

$$\beta[\sigma(\mathbf{r})+\sigma(\mathbf{r}')]-\frac{1}{N_c^2-1}(1-\beta)\Delta\Sigma_{88}(\mathbf{r},\mathbf{r}') =$$
$$=\frac{N_c^2\beta-1}{N_c^2-1}[\sigma(\mathbf{r})+\sigma(\mathbf{r}')], \quad (61)$$

and it is advisable to work with the perturbative expansion in (59).

The final result for the nuclear absorption factor to the accuracy $1/(N_c^2-1)$ is given by

$$D_A(\mathbf{s},\mathbf{r},\mathbf{r}',\mathbf{b}) = D_A^{(1)}(\mathbf{s},\mathbf{r},\mathbf{r}',\mathbf{b}) + D_A^{(2)}(\mathbf{s},\mathbf{r},\mathbf{r}',\mathbf{b}) +$$
$$+ D_A^{(3)}(\mathbf{s},\mathbf{r},\mathbf{r}',\mathbf{b}) + D_A^{(4)}(\mathbf{s},\mathbf{r},\mathbf{r}',\mathbf{b}) + D_A^{(5)}(\mathbf{s},\mathbf{r},\mathbf{r}',\mathbf{b}),$$

where

$$D_A^{(1)}(\mathbf{s},\mathbf{r},\mathbf{r}',\mathbf{b}) = \frac{\Sigma_{18}(\mathbf{s},\mathbf{r},\mathbf{r}')T^(\mathbf{b})}{2(N_c^2-1)}\int_0^1 d\beta\int_0^\beta d\beta_1\times$$
$$\times\exp\left\{-\frac{1}{2}(1-\beta+\beta_1)[\sigma(\mathbf{r})+\sigma(\mathbf{r}')]T(\mathbf{b})\right\}\times$$
$$\times\exp\left\{-\frac{1}{2}(\beta-\beta_1)[\sigma(\mathbf{s})+\sigma(\mathbf{s}-\mathbf{r}+\mathbf{r}')]T(\mathbf{b})\right\}, \quad (62)$$

$$D_A^{(2)}(\mathbf{s},\mathbf{r},\mathbf{r}',\mathbf{b}) = \frac{\Sigma_{18}^2(\mathbf{s},\mathbf{r},\mathbf{r}')T^2(\mathbf{b})}{4(N_c^2-1)}\int_0^1 d\beta\int_0^\beta d\beta_1\times$$
$$\times\int_0^{\beta_1} d\beta_2\exp\left\{-\frac{1}{2}(\beta-\beta_1+\beta_2)[\sigma(\mathbf{r})+\sigma(\mathbf{r}')]T(\mathbf{b})\right\}\times$$
$$\times\exp\left\{-\frac{1}{2}(1-\beta+\beta_1-\beta_2)\times\right.$$
$$\left.\times[\sigma(\mathbf{s})+\sigma(\mathbf{s}-\mathbf{r}+\mathbf{r}')]T(\mathbf{b})\right\}, \quad (63)$$

$$D_A^{(3)}(\mathbf{s},\mathbf{r},\mathbf{r}',\mathbf{b}) = -\frac{\Sigma_{18}(\mathbf{s},\mathbf{r},\mathbf{r}')T(\mathbf{b})}{N_c^2-1}\int_0^1 d\beta(1-\beta)\times$$
$$\times\exp\left\{-\frac{1}{2}\beta[\sigma(\mathbf{r})+\sigma(\mathbf{r}')]T(\mathbf{b})\right\}\times$$
$$\times\exp\left\{-\frac{1}{2}(1-\beta)\lambda_c[\sigma(\mathbf{s})+\sigma(\mathbf{s}-\mathbf{r}+\mathbf{r}')]T(\mathbf{b})\right\}, \quad (64)$$

$$D_A^{(4)}(\mathbf{s},\mathbf{r},\mathbf{r}',\mathbf{b}) = \frac{\Delta\Sigma_{88}(\mathbf{r},\mathbf{r}')T(\mathbf{b})}{2(N_c^2-1)}\int_0^1 d\beta(1-\beta)\times$$
$$\times\exp\left\{-\frac{1}{2}\beta[\sigma(\mathbf{r})+\sigma(\mathbf{r}')]T(\mathbf{b})\right\}\times$$
$$\times\exp\left\{-\frac{1}{2}(1-\beta)\lambda_c[\sigma(\mathbf{s})+\sigma(\mathbf{s}-\mathbf{r}+\mathbf{r}')]T(\mathbf{b})\right\}, \quad (65)$$

$$D_A^{(5)}(\mathbf{s},\mathbf{r},\mathbf{r}',\mathbf{b}) =$$
$$=\int_0^1 d\beta\exp\left\{-\frac{1}{2}(1-\beta)[\sigma(\mathbf{r})+\sigma(\mathbf{r}')]T(\mathbf{b})\right\}\times$$
$$\times\exp\left\{-\frac{1}{2}\beta[\sigma(\mathbf{s})+\sigma(\mathbf{s}+\mathbf{r}'-\mathbf{r})]T(\mathbf{b})\right\}. \quad (66)$$

Equation (66) is the leading large-N_c result, Eqs. (62) and (63) describe contributions to the dijet cross section of the second and third order in the off-diagonal matrix element σ_{18}, and Eqs. (64) and (65) come from expansion (59).

As an illustration of salient features of the $1/(N_c^2-1)$-corrections, we expose the contribution from the first term (62) in detail. Following the considerations in Secs. 4 and 5, we readily obtain

$$\frac{d\Delta\sigma_{in}^{(1)}}{d\mathbf{b}\,dz\,d\mathbf{p}_-d\boldsymbol{\Delta}}=\frac{\alpha_S^2\sigma_0^2T^2(\mathbf{b})}{4(2\pi)^2(N_c^2-1)}\int\limits_0^1 d\beta\int\limits_0^\beta d\beta_1\times$$
$$\times\int d\mathbf{q}_1d\mathbf{q}_2d\boldsymbol{\kappa}_3f(\mathbf{q}_1)f(\mathbf{q}_2)\times$$
$$\times\Phi((\beta-\beta_1)\nu_A(\mathbf{b}),\boldsymbol{\Delta}-\boldsymbol{\kappa}_3-\mathbf{q}_1-\mathbf{q}_2)\times$$
$$\times\Phi((\beta-\beta_1)\nu_A(\mathbf{b}),\boldsymbol{\kappa}_3)\times$$
$$\times\left|\int d\boldsymbol{\kappa}_1\Phi((1-\beta+\beta_1)\nu_A(\mathbf{b}),\boldsymbol{\kappa}_1)\times\right.$$
$$\times\Big\{\langle\gamma^*|z,\mathbf{p}_-+\boldsymbol{\kappa}_1+\boldsymbol{\kappa}_3\rangle-\langle\gamma^*|z,\mathbf{p}_-+\boldsymbol{\kappa}_1+\boldsymbol{\kappa}_3+\mathbf{q}_1\rangle-$$
$$-\langle\gamma^*|z,\mathbf{p}_-+\boldsymbol{\kappa}_1+\boldsymbol{\kappa}_3+\mathbf{q}_2\rangle+$$
$$\left.+\langle\gamma^*|z,\mathbf{p}_-+\boldsymbol{\kappa}_1+\boldsymbol{\kappa}_3+\mathbf{q}_1+\mathbf{q}_2\rangle\Big\}\right|^2. \quad (67)$$

Of particular interest is the large-$|\mathbf{p}_-|$ behavior of (67). We note that for $\mathbf{p}_-^2\gg Q_A^2(\mathbf{b})$, we can neglect $\boldsymbol{\kappa}_{1,3}$ in the argument of the photon wave function, and hence

$$\int d\boldsymbol{\kappa}_1\Phi((1-\beta+\beta_1)\nu_A(\mathbf{b}),\boldsymbol{\kappa}_1)\times$$
$$\times\Big\{\langle\gamma^*|z,\mathbf{p}_-+\boldsymbol{\kappa}_1+\boldsymbol{\kappa}_3\rangle-\langle\gamma^*|z,\mathbf{p}_-+\boldsymbol{\kappa}_1+\boldsymbol{\kappa}_3+\mathbf{q}_1\rangle-$$
$$-\langle\gamma^*|z,\mathbf{p}_-+\boldsymbol{\kappa}_1+\boldsymbol{\kappa}_3+\mathbf{q}_2\rangle+$$
$$+\langle\gamma^*|z,\mathbf{p}_-+\boldsymbol{\kappa}_1+\boldsymbol{\kappa}_3+\mathbf{q}_1+\mathbf{q}_2\rangle\Big\}\approx$$
$$\approx\Big\{\langle\gamma^*|z,\mathbf{p}_-\rangle-\langle\gamma^*|z,\mathbf{p}_-+\mathbf{q}_1\rangle-\langle\gamma^*|z,\mathbf{p}_-+\mathbf{q}_2\rangle+$$
$$+\langle\gamma^*|z,\mathbf{p}_-+\mathbf{q}_1+\mathbf{q}_2\rangle\Big\}, \quad (68)$$

where we used the normalization property

$$\int d\boldsymbol{\kappa}_1\Phi((1-\beta+\beta_1)\nu_A(\mathbf{b}),\boldsymbol{\kappa}_1)=1.$$

Next, we can readily verify that

$$\int d\boldsymbol{\kappa}_3\Phi((\beta-\beta_1)\nu_A(\mathbf{b}),\boldsymbol{\Delta}-\boldsymbol{\kappa}_3-\mathbf{q}_1-\mathbf{q}_2)\times$$
$$\times\Phi((\beta-\beta_1)\nu_A(\mathbf{b}),\boldsymbol{\kappa}_3)=$$
$$=\Phi((\beta-\beta_1)\nu_A(\mathbf{b}),\boldsymbol{\Delta}-\mathbf{q}_1-\mathbf{q}_2). \quad (69)$$

Incidentally, by a similar analysis of the onset of the high-$\mathbf{p}_+$ limit, one would obtain the linear nuclear $k_\perp$-factorization (36) for hard dijets from the nonlinear nuclear $k_\perp$-factorization (41).

The combination of the photon wave functions in (68) corresponds to the second finite difference in $\mathbf{q}_1$ and $\mathbf{q}_2$, and therefore for jets with $\mathbf{p}_-^2\gg\varepsilon^2$, we have the estimate

$$\Big|\langle\gamma^*|z,\mathbf{p}_-\rangle-\langle\gamma^*|z,\mathbf{p}_-+\mathbf{q}_1\rangle+\langle\gamma^*|z,\mathbf{p}_-+\mathbf{q}_2\rangle-$$
$$-\langle\gamma^*|z,\mathbf{p}_-+\mathbf{q}_1+\mathbf{q}_2\rangle\Big|^2\approx\Big|\langle\gamma^*|z,\mathbf{p}_-\rangle\Big|^2\frac{\mathbf{q}_1^2\mathbf{q}_2^2}{(\mathbf{p}_-^2)^2}, \quad (70)$$

which shows that the contribution to the dijet cross section from terms of the second order in σ_{18}^2 is the higher twist correction. Compared to the leading large-N_c cross section, it contains extra $\int d\mathbf{q}_2\,\mathbf{q}_2^2f(\mathbf{q}_2)$ and an extra power of $\alpha_S\sigma_0T(\mathbf{b})$, which combine to precisely the dimensional nuclear saturation scale $Q_A^2(\mathbf{b})$, see Eq. (52), such that the resulting suppression factor is

$$\frac{d\Delta\sigma_{in}^{(1)}}{d\sigma_{in}}\sim\frac{1}{(N_c^2-1)}\,\frac{Q_A^2(\mathbf{b})}{\mathbf{p}_-^2}. \quad (71)$$

As far as the expansion in higher inverse powers of the hard scale $\mathbf{p}_-^2$ is concerned, $\Delta\sigma_{in}^{(1)}$ has the form of a higher twist correction. In the retrospect, we observe that the principal approximation (68) in the above derivation for hard dijets amounts to putting $|\mathbf{r}|,|\mathbf{r}'|\ll|\mathbf{s}|$ in the attenuation factors in the β,β_1 integrand in (62). But the exact $\mathbf{r},\mathbf{r}'$-dependence must be retained in the prefactor $\Sigma_{18}(\mathbf{s},\mathbf{r},\mathbf{r}')$, because it vanishes if either $\mathbf{r}=0$ or $\mathbf{r}'=0$. It is precisely the latter property that provides the finite-difference structure of the combination of the photon wave functions in (67) and (68) and is behind the higher twist property (71) of the $1/(N_c^2-1)$-correction.

The second term, Eq. (63), gives the correction

$$\frac{d\Delta\sigma_{in}^{(2)}}{d\mathbf{b}\,dz\,d\mathbf{p}_-d\boldsymbol{\Delta}}=\frac{\alpha_S^3\sigma_0^3T^3(\mathbf{b})}{8(2\pi)^2(N_c^2-1)}\int\limits_0^1 d\beta\int\limits_0^\beta d\beta_1\times$$
$$\times\int\limits_0^{\beta_1}d\beta_2\int d\mathbf{q}_1d\mathbf{q}_2d\mathbf{q}_3d\boldsymbol{\kappa}_3f(\mathbf{q}_1)f(\mathbf{q}_2)f(\mathbf{q}_3)\times$$
$$\times\Phi((1-\beta+\beta_1-\beta_2)\nu_A(\mathbf{b}),\boldsymbol{\Delta}-\boldsymbol{\kappa}_3-\mathbf{q}_1-\mathbf{q}_2-\mathbf{q}_3)\times$$
$$\times\Phi((1-\beta+\beta_1-\beta_2)\nu_A(\mathbf{b}),\boldsymbol{\kappa}_3)\times$$
$$\times\left|\int d\boldsymbol{\kappa}_1\Phi((\beta-\beta_1+\beta_2)\nu_A(\mathbf{b}),\boldsymbol{\kappa}_1)\times\right.$$
$$\times\Big\{\langle\gamma^*|z,\mathbf{p}_-+\boldsymbol{\kappa}_1+\boldsymbol{\kappa}_3\rangle-\langle\gamma^*|z,\mathbf{p}_-+\boldsymbol{\kappa}_1+\boldsymbol{\kappa}_3+\mathbf{q}_1\rangle-$$
$$-\langle\gamma^*|z,\mathbf{p}_-+\boldsymbol{\kappa}_1+\boldsymbol{\kappa}_3+\mathbf{q}_2\rangle+\langle\gamma^*|z,\mathbf{p}_-+\boldsymbol{\kappa}_1+\boldsymbol{\kappa}_3+\mathbf{q}_1+\mathbf{q}_2\rangle-$$
$$-\langle\gamma^*|z,\mathbf{p}_-+\boldsymbol{\kappa}_1+\boldsymbol{\kappa}_3+\mathbf{q}_3\rangle+\langle\gamma^*|z,\mathbf{p}_-+\boldsymbol{\kappa}_1+\boldsymbol{\kappa}_3+\mathbf{q}_3+\mathbf{q}_1\rangle+$$
$$+\langle\gamma^*|z,\mathbf{p}_-+\boldsymbol{\kappa}_1+\boldsymbol{\kappa}_3+\mathbf{q}_3+\mathbf{q}_2\rangle-$$
$$\left.-\langle\gamma^*|z,\mathbf{p}_-+\boldsymbol{\kappa}_1+\boldsymbol{\kappa}_3+\mathbf{q}_1+\mathbf{q}_2+\mathbf{q}_3|\gamma^*\rangle\Big\}\right|^2. \quad (72)$$

The combination of the photon wave functions in (72) corresponds to the third finite derivative in $\mathbf{q}_{1,2,3}$. Starting from (72), we can readily repeat the analysis that leads to estimate (71). Alternatively, we can take the simplified form of the attenuation factors, as explained below Eq. (71). Either way, we find that the contribution from third-order terms in σ_{18} is of an even higher twist and has the smallness

$$\frac{d\Delta\sigma_{in}^{(2)}}{d\sigma_{in}} \sim \frac{1}{N_c^2-1}\left(\frac{Q_A^2(\mathbf{b})}{\mathbf{p}_-^2}\right)^2. \qquad (73)$$

Apart from a slight difference in the structure of the β integrations, correction (64) is not different from $d\Delta\sigma^{(1)}$ in Eq. (68),

$$\frac{d\Delta\sigma_{in}^{(3)}}{d\mathbf{b}\,dz\,d\mathbf{p}_-d\boldsymbol{\Delta}} = -\frac{\alpha_S^2\sigma_0^2T^2(\mathbf{b})}{4(2\pi)^2(N_c^2-1)}\int_0^1 d\beta(1-\beta)\times$$
$$\times\int d\mathbf{q}_1d\mathbf{q}_2d\boldsymbol{\kappa}_3 f(\mathbf{q}_1)f(\mathbf{q}_2)\times$$
$$\times\,\Phi((1-\beta)\lambda_c\nu_A(\mathbf{b}),\boldsymbol{\Delta}-\boldsymbol{\kappa}_3-\mathbf{q}_1-\mathbf{q}_2)\times$$
$$\times\,\Phi((1-\beta)\lambda_c\nu_A(\mathbf{b}),\boldsymbol{\kappa}_3)\times$$
$$\times\left|\int d\boldsymbol{\kappa}_1\Phi(\beta)\nu_A(\mathbf{b}),\boldsymbol{\kappa}_1)\times\right.$$
$$\times\Big\{\langle\gamma^*|z,\gamma^*|z,\mathbf{p}_-+\boldsymbol{\kappa}_1+\boldsymbol{\kappa}_3\rangle-\langle\gamma^*|z,\gamma^*|z,\mathbf{p}_-+\boldsymbol{\kappa}_1+\boldsymbol{\kappa}_3+\mathbf{q}_1\rangle-$$
$$-\langle\gamma^*|z,\gamma^*|z,\mathbf{p}_-+\boldsymbol{\kappa}_1+\boldsymbol{\kappa}_3+\mathbf{q}_2\rangle+$$
$$\left.+\langle\gamma^*|z,\mathbf{p}_-+\boldsymbol{\kappa}_1+\boldsymbol{\kappa}_3+\mathbf{q}_1+\mathbf{q}_2\rangle\Big\}\right|^2. \qquad (74)$$

Consequently, the same estimate (71) is also valid for $d\Delta\sigma^{(3)}$.

The correction $d\Delta\sigma^{(4)}$ requires a bit more scrutiny. It contains a product of the first and second finite derivatives of the photon wave function,

$$\frac{d\Delta\sigma_{in}^{(4)}}{d\mathbf{b}\,dz\,d\mathbf{p}_-d\boldsymbol{\Delta}} = \frac{\alpha_S^2\sigma_0^2T^2(\mathbf{b})}{2(2\pi)^2(N_c^2-1)}\int_0^1 d\beta(1-\beta)\times$$
$$\times\int d\mathbf{q}_1d\mathbf{q}_2d\boldsymbol{\kappa}_1d\boldsymbol{\kappa}_2d\boldsymbol{\kappa}_3 f(\mathbf{q}_1)f(\mathbf{q}_2)\Phi(\beta\nu_A(\mathbf{b}),\boldsymbol{\kappa}_1)\times$$
$$\times\,\Phi(\beta\nu_A(\mathbf{b}),\boldsymbol{\kappa}_2)\times$$
$$\times\,\Phi((1-\beta)\lambda_c\nu_A(\mathbf{b}),\boldsymbol{\Delta}-\boldsymbol{\kappa}_3-\mathbf{q}_1-\mathbf{q}_2)\times$$
$$\times\,\Phi((1-\beta)\lambda_c\nu_A(\mathbf{b}),\boldsymbol{\kappa}_3)\times$$
$$\times\Big\{\langle\gamma^*|z,\gamma^*|z,\mathbf{p}_-+\boldsymbol{\kappa}_1+\boldsymbol{\kappa}_3\rangle-$$
$$-\langle\gamma^*|z,\gamma^*|z,\mathbf{p}_-+\boldsymbol{\kappa}_1+\boldsymbol{\kappa}_3+\mathbf{q}_1\rangle\Big\}\times$$
$$\times\Big\{\langle\gamma^*|z,\mathbf{p}_-+\boldsymbol{\kappa}_1+\boldsymbol{\kappa}_3\rangle-\langle\gamma^*|z,\mathbf{p}_-+\boldsymbol{\kappa}_1+\boldsymbol{\kappa}_3+\mathbf{q}_1\rangle-$$
$$-\langle\gamma^*|z,\mathbf{p}_-+\boldsymbol{\kappa}_1+\boldsymbol{\kappa}_3+\mathbf{q}_2\rangle+$$
$$+\langle\gamma^*|z,\mathbf{p}_-+\boldsymbol{\kappa}_1+\boldsymbol{\kappa}_3+\mathbf{q}_1+\mathbf{q}_2\rangle\Big\}, \qquad (75)$$

and in the interesting case of hard dijets,

$$\frac{d\Delta\sigma_{in}^{(4)}}{d\mathbf{b}\,dz\,d\mathbf{p}_-d\boldsymbol{\Delta}} = \frac{\alpha_S^2\sigma_0^2T^2(\mathbf{b})}{2(2\pi)^2(N_c^2-1)}\int_0^1 d\beta(1-\beta)\times$$
$$\times\int d\mathbf{q}_1d\mathbf{q}_2 f(\mathbf{q}_1)f(\mathbf{q}_2)\Phi(2(1-\beta)\lambda_c\nu_A(\mathbf{b}),\boldsymbol{\Delta}-\mathbf{q}_1-\mathbf{q}_2)\times$$
$$\times\Big\{\langle\gamma^*|z,\gamma^*|z,\mathbf{p}_-\rangle-\langle\gamma^*|z,\gamma^*|z,\mathbf{p}_-+\mathbf{q}_1\rangle\Big\}\times$$
$$\times\Big\{\langle\gamma^*|z,\mathbf{p}_-\rangle-\langle\gamma^*|z,\mathbf{p}_-+\mathbf{q}_1\rangle-$$
$$-\langle\gamma^*|z,\mathbf{p}_-+\mathbf{q}_2\rangle+\langle\gamma^*|z,\mathbf{p}_-+\mathbf{q}_1+\mathbf{q}_2\rangle\Big\}. \qquad (76)$$

The leading term of the small-$\mathbf{q}_{1,2}$ expansion of the product of the photon wave functions in (74) is a quadratic function of $\mathbf{q}_1$ and a linear function of $\mathbf{q}_2$ of the form

$$|\langle\gamma^*|z,\mathbf{p}_-\rangle|^2\frac{(\mathbf{p}_-\cdot\mathbf{q}_1)^2(\mathbf{p}_-\cdot\mathbf{q}_2)}{p_-^6}. \qquad (77)$$

The leading nonvanishing term comes from the expansion of the nuclear WW glue,

$$\Phi(2(1-\beta)\lambda_c\nu_A(\mathbf{b}),\boldsymbol{\Delta}-\mathbf{q}_1-\mathbf{q}_2)-$$
$$-\Phi(2(1-\beta)\lambda_c\nu_A(\mathbf{b}),\boldsymbol{\Delta})\sim$$
$$\sim\Phi(2(1-\beta)\lambda_c\nu_A(\mathbf{b}),\boldsymbol{\Delta})\times$$
$$\times\frac{\boldsymbol{\Delta}\cdot(\mathbf{q}_1+\mathbf{q}_2)}{2(1-\beta)\lambda_cQ_A^2(\mathbf{b})+\boldsymbol{\Delta}^2}. \qquad (78)$$

Namely, upon the azimuthal averaging of (77) in conjunction with (78), we find the leading nonvanishing term of the form $2(\mathbf{p}_-\mathbf{q}_2)(\boldsymbol{\Delta}\mathbf{q}_2)\to(\mathbf{p}_-\boldsymbol{\Delta})\mathbf{q}_2^2$, and therefore

$$\frac{d\Delta\sigma_{in}^{(4)}}{d\sigma_{in}} \sim \frac{1}{N_c^2-1}\,\frac{\mathbf{p}_-\cdot\boldsymbol{\Delta}}{\mathbf{p}_-^2}, \qquad (79)$$

which is reminiscent of a higher twist-3 correction.

To summarize, nonlinear nuclear $k_\perp$-factorization allows a consistent evaluation of the $1/N_c^2$-corrections. We demonstrated how the expansion in $1/(N_c^2-1)$ comes along with a higher twist expansion. One exception is the reabsorption of one of the terms proportional to $1/(N_c^2-1)$ in σ_{88} into the renormalization of the leading term in σ_{88} by the N_c-dependent factor λ_c. We conclude this discussion by a comment that all the arguments in Sec. 5 regarding the disappearance of azimuthal correlations of minijets hold for the $1/N_c^2$-corrections as well.

8. SUMMARY AND CONCLUSIONS

We formulated the theory of the breakup of photons into dijets in DIS off nuclear targets based on the consistent treatment of propagation of color dipoles in nuclear medium. The non-Abelian intranuclear evolution of color dipoles gives rise to a nontrivial spectrum of the attenuation eigenvalues, but the familiar Glauber–Gribov multiple-scattering results are recovered for the nuclear total cross sections. However, in more special cases like DIS in which the photon breaks up into color-singlet dijets, the cross section depends on the complete spectrum of the attenuation eigenstates.

We derived the nuclear broadening of the acoplanarity momentum distribution in the breakup of photons into dijets, see Eqs. (35) and (41). Our principal finding is that all nuclear DIS observables — the amplitude of coherent diffractive breakup into dijets [6], nuclear sea quark SF and its decomposition into equally important genuine inelastic and diffractive components performed in [5], and the jet–jet inclusive cross section derived in the present paper — are uniquely calculable in terms of the NSS-defined collective nuclear WW glue. This property can be regarded as a nuclear $k_\perp$-factorization theorem that connects DIS in the regimes of low and high density of partons. For the generic dijet cross section, nuclear $k_\perp$-factorization is of a highly nonlinear form, which must be contrasted to the linear hard factorization for the free nucleon target. This result is derived to the leading order in large N_c; the further evaluation of the $1/N_c^2$-corrections shows a close relation between the $1/N_c^2$ and high-twist expansions. Furthermore, the $1/N_c^2$-corrections themselves admit the nonlinear nuclear $k_\perp$-factorization representation.

We demonstrated the disappearance of azimuthal jet–jet correlations of minijets with momenta below the saturation scale. Based on the ideas on generalization of the dipole picture to hadron–nucleus collisions [17,18], we presented qualitative estimates of the broadening effect for mid-rapidity jets produced in central nucleus–nucleus collisions and argued that our azimuthal decorrelation may contribute substantially to the disappearance of back-to-back high-$p_\perp$ hadron correlation in central gold–gold collisions observed by the STAR collaboration at RHIC [20].

We conclude by the comment that all the results for hard single-jet and jet–jet inclusive cross sections can be readily extended from DIS to the breakup of projectile hadrons into forward jets. Indeed, as argued in [6], the final state interaction between the final state quark and antiquark can be neglected and the plane-wave approximation becomes applicable as soon as the invariant mass of the forward jet system exceeds a typical mass scale of prominent meson and baryon resonances. Here, we confine ourselves to the statement that although our principal point about a nonlinear nuclear $k_\perp$-factorization is fully retained, we find important distinctions between the breakup of pointlike photons and nonpointlike hadrons

This work has been partly supported by the INTAS (grants Nos. 97-30494 and 00-00366) and the DFG (grant No. 436RUS17/119/02).

APPENDIX A

Calculation of the 4-body color dipole cross section

The Feynman diagrams for the matrix of 4-parton dipole cross section $\sigma_4(\mathbf{s},\mathbf{r},\mathbf{r}')$, Eqs. (19)–(21), are shown in Fig. 2. The profile function for the color-singlet $q\bar{q}$ pair is given by the diagrams in Figs. 2*a–d*,

$$
\begin{aligned}
2\Gamma(\text{Figs. } 2a\text{–}d;(q\bar{q})_1 N;\mathbf{b}_+,\mathbf{b}_-) &= \\
&= \frac{1}{N_c}\delta_{ab}\left\{[\chi^2(\mathbf{b}_+)+\chi^2(\mathbf{b}_-)]\mathrm{Tr}(T^aT^b) - \right. \\
&\quad \left. - 2\chi(\mathbf{b}_+)\chi(\mathbf{b}_-)\mathrm{Tr}(T^aT^b)\right\} = \\
&= \frac{N_c^2-1}{2N_c}[\chi(\mathbf{b}_+)-\chi(\mathbf{b}_-)]^2\,, \qquad (80)
\end{aligned}
$$

which has already been cited in the main text, Eq. (11). Upon adding the contribution from diagrams in Figs. 2*e–h*, we obtain the obvious result in Eq. (19).

The color-diagonal contribution of the same dia-

grams to the interaction of the color-octet $q\bar{q}$ pair with the nucleon is given by

$$2\Gamma(\text{Figs. } 2a\text{–}d;(q\bar{q})_8 N;\mathbf{b}_+,\mathbf{b}_-) = \\ = \frac{2}{N_c^2-1}\delta_{ab}\left\{[\chi^2(\mathbf{b}_+)+\chi^2(\mathbf{b}_-)]\mathrm{Tr}(T^cT^aT^bT^c) - \right. \\ \left. -2\chi(\mathbf{b}_+)\chi(\mathbf{b}_-)\mathrm{Tr}(T^cT^aT^cT^b)\right\} = \frac{N_c^2-1}{2N_c}\times \\ \times\left\{\left[\chi^2(\mathbf{b}_+)+\chi^2(\mathbf{b}_-)\right]+\frac{2}{N_c^2-1}\chi(\mathbf{b}_+)\chi(\mathbf{b}_-)\right\}. \quad (81)$$

The contribution to the matrix element $\langle 88|\sigma_4|88\rangle$ from color-diagonal interactions of the $q'\bar{q}'$ pair is obtained from (81) by the substitution $\mathbf{b}_\pm \to \mathbf{b}'_\pm$,

$$\Gamma_4(\text{Figs. } 2a\text{–}d+\text{Figs. } 2e\text{–}h;(88)N;\mathbf{b}_+,\mathbf{b}_-,\mathbf{b}'_+,\mathbf{b}'_-) = \\ = \Gamma(\text{Figs. } 2a\text{–}d;q\bar{q})_8 N;\mathbf{b}_+,\mathbf{b}_-) + \\ + \Gamma(\text{Figs. } 2a\text{–}d;q\bar{q})_8 N;\mathbf{b}'_+,\mathbf{b}'_-). \quad (82)$$

The diagrams in Figs. $2i$–l describe processes with color-space rotation of the $q\bar{q}$ pair,

$$2\Gamma_4(\text{Figs. } 2i\text{–}l;(88)N\to(88)N;\mathbf{b}_+,\mathbf{b}_-,\mathbf{b}'_+,\mathbf{b}'_-) = \\ = \frac{8}{N_c^2-1}\delta_{ab}\left\{\left[\chi(\mathbf{b}_+)\chi(\mathbf{b}'_-)+\chi(\mathbf{b}_-)\chi(\mathbf{b}'_+)\right]\times\right. \\ \times\mathrm{Tr}(T^cT^aT^d)\mathrm{Tr}(T^cT^bT^d) - \\ \left. -\left[\chi(\mathbf{b}_+)\chi(\mathbf{b}'_+)+\chi(\mathbf{b}_-)\chi(\mathbf{b}'_-)\right]\times\right. \\ \left.\times\,\mathrm{Tr}(T^cT^aT^d)\mathrm{Tr}(T^dT^bT^c)\right\} = \\ = -\frac{N_c^2-1}{N_c}\left\{\frac{2}{N_c^2-1}\left[\chi(\mathbf{b}_+)\chi(\mathbf{b}'_-)+\chi(\mathbf{b}_-)\chi(\mathbf{b}'_+)\right]+\right. \\ \left.+\frac{N_c^2-2}{N_c^2-1}\left[\chi(\mathbf{b}_+)\chi(\mathbf{b}'_+)+\chi(\mathbf{b}_-)\chi(\mathbf{b}'_-)\right]\right\}. \quad (83)$$

The $(11)N \to (88)N$ transition matrix element comes from the diagrams in Figs. $2i$–l,

$$2\Gamma_4(\text{Figs. } 2i\text{–}l;(11)N\to(88)N;\mathbf{b}_+,\mathbf{b}_-,\mathbf{b}'_+,\mathbf{b}'_-) = \\ = \frac{4}{N_c\sqrt{N_c^2-1}}\delta_{ab}\left\{\left[\chi(\mathbf{b}_+)\chi(\mathbf{b}'_-)+\chi(\mathbf{b}_-)\chi(\mathbf{b}'_+)\right]\times\right. \\ \times\mathrm{Tr}(T^cT^a)\mathrm{Tr}(T^cT^b) - \\ \left. -\left[\chi(\mathbf{b}_+)\chi(\mathbf{b}'_+)+\chi(\mathbf{b}_-)\chi(\mathbf{b}'_-)\right]\mathrm{Tr}(T^cT^a)\mathrm{Tr}(T^cT^b)\right\} = \\ = \frac{N_c^2-1}{N_c}\frac{1}{\sqrt{N_c^2-1}}\left\{\left[\chi(\mathbf{b}_+)\chi(\mathbf{b}'_-)+\chi(\mathbf{b}_-)\chi(\mathbf{b}'_+)\right]-\right. \\ \left.-\left[\chi(\mathbf{b}_+)\chi(\mathbf{b}'_+)+\chi(\mathbf{b}_-)\chi(\mathbf{b}'_-)\right]\right\}. \quad (84)$$

Upon the rearrangement

$$-2\chi(\mathbf{b}_i)\chi(\mathbf{b}_j) = [\chi(\mathbf{b}_i)-\chi(\mathbf{b}_j)]^2-\chi^2(\mathbf{b}_i)-\chi^2(\mathbf{b}_j),$$

we can readily verify that the terms proportional to $\chi^2(\mathbf{b}_i)$ cancel each other, and the 4-body cross section matrix contains only linear combinations of $\sigma(\mathbf{b}_i-\mathbf{b}_j)$, recall a discussion in [24].

APPENDIX B

Non-Abelian vs. Abelian aspects of intranuclear propagation of color dipoles and the Glauber–Gribov formalism

The intranuclear propagation of color-octet $q\bar{q}$ pairs is part and parcel of the complete formalism for DIS off nucleus. It is interesting to recover the quasi-Abelian color-dipole results for the nuclear cross sections [13, 14] that are of the Glauber–Gribov form [21, 22]. We first consider the total inelastic cross section obtained from (8) upon the integration over the transverse momenta $\mathbf{p}_\pm$ of the quark and antiquark, which amounts to putting $\mathbf{b}_+ = \mathbf{b}'_+$ and $\mathbf{b}_- = \mathbf{b}'_-$. Then we are left with the system of two color dipoles of the same size $\mathbf{r} = \mathbf{b}_+ - \mathbf{b}_- = \mathbf{r}' = \mathbf{b}'_+ - \mathbf{b}'_-$, and the matrix of the 4-body cross section has the eigenvalues

$$\Sigma_1 = 0, \quad (85)$$

$$\Sigma_2 = \frac{2N_c^2}{N_c^2-1}\sigma(\mathbf{r}) \quad (86)$$

with the eigenstates

$$|f_1\rangle = \frac{1}{N_c}(|11\rangle + \sqrt{N_c^2-1}|88\rangle), \quad (87)$$

$$|f_2\rangle = \frac{1}{N_c}(\sqrt{N_c^2-1}|11\rangle - |88\rangle). \quad (88)$$

The existence of the nonattenuating 4-quark state with $\Sigma_1 = 0$ is quite obvious and corresponds to an overlap of two $q\bar{q}$ dipoles of the same size with neutralization of color charges. The existence of such a nonattenuating state is shared by an Abelian and non-Abelian quark–gluon interaction. The intranuclear attenuation eigen-cross section (86) differs from $\sigma(\mathbf{r})$ for the color-singlet $q\bar{q}$ pair by the nontrivial color factor

$$2\lambda_c = 2N_c^2/(N_c^2-1) = C_A/C_F,$$

which occurs because the relevant 4-parton state is in the color octet–(anti)octet configuration.

The crucial point is that the final state that enters the calculation of the genuine inelastic DIS off a nucleus, see Eq. (15), is precisely the eigenstate $|f_1\rangle$. Then, even without invoking Sylvester expansion (23)

and (25), the straightforward result for the inelastic cross section is

$$\sigma_{in} = \int d\mathbf{r}\, dz\, |\Psi(Q^2, z, \mathbf{r})|^2 \int d\mathbf{b} \times$$
$$\times \left\{ N_c \langle f_1 | \exp\left[-\frac{1}{2}\sigma_4 T(\mathbf{b})\right] |11\rangle - \exp\left[-\sigma(\mathbf{r})T(\mathbf{b})\right] \right\} =$$
$$= \int d\mathbf{b} \langle \gamma^* | \left\{ \exp\left[-\frac{1}{2}\Sigma_1 T(\mathbf{b})\right] - \exp\left[-\sigma(\mathbf{r})T(\mathbf{b})\right] \right\} \times$$
$$\times |\gamma^*\rangle = \int d\mathbf{b} \langle \gamma^* | \left\{1 - \exp\left[-\sigma(\mathbf{r})T(\mathbf{b})\right]\right\} |\gamma^*\rangle, \quad (89)$$

which is precisely the color-dipole generalization [14] of the Glauber–Gribov formula [21, 22] in which no trace of a non-Abelian intranuclear evolution with the nontrivial attenuation eigenstate (88) with eigen-cross section (86) is left.

When the photon breaks into a color-singlet $q\bar{q}$ dijet, the net flow of color between the $q\bar{q}$ pair and color-excited debris of the target nucleus is zero. This suggests that a rapidity gap can survive hadronization, although whether the rapidity gap in genuine inelastic events with the color-singlet $q\bar{q}$ production is stable against higher-order corrections remains an interesting open issue. Although the debris of the target nucleus have zero net color charge, the debris of color-excited nucleons are spatially separated by a distance of the order of the nuclear radius, which suggests the total excitation energy of the order of 1 GeV times $A^{1/3}$, such that such rapidity-gap events look like a double diffraction with multiple production of mesons in the nucleus fragmentation region (see [36] for the theoretical discussion of conventional mechanisms of diffraction excitation of nuclei in proton–nucleus collisions; the experimental observation has been reported in [37]). As such, inelastic excitation of color-singlet dijets is distinguishable from quasielastic diffractive DIS followed by excitation and breakup of the target nucleus without production of secondary particles.

Using the Sylvester expansion (23)–(25) and eigenstates (87) and (88), we readily obtain

$$\sigma_{in}(A^*(q\bar{q})_1) = \int d\mathbf{b} \times$$
$$\times \langle \gamma^* | \left\{ 1 - \exp\left[-\sigma(\mathbf{r})T(\mathbf{b})\right] - \right.$$
$$\left. - \frac{N_c^2 - 1}{N_c^2} \left(1 - \exp\left[-\frac{1}{2}\Sigma_2 T(\mathbf{b})\right] \right) \right\} |\gamma^*\rangle, \quad (90)$$

$$\sigma_{in}(A^*(q\bar{q})_8) = \frac{N_c^2 - 1}{N_c^2} \times$$
$$\times \int d\mathbf{b} \langle \gamma^* | \left\{ 1 - \exp\left[-\frac{1}{2}\Sigma_2 T(\mathbf{b})\right] \right\} |\gamma^*\rangle. \quad (91)$$

These expressions depend on the entire non-Abelian spectrum of attenuation eigenstates.

Several features of the result in (90) are noteworthy. First, the color neutralization of the $q\bar{q}$ pair after the first inelastic interaction requires at least one more secondary inelastic interaction, and the expansion of the integrand of $\sigma_{in}(A^*(q\bar{q})_1)$ starts with the term quadratic in the optical thickness,

$$\left\{ 1 - \exp\left[-\sigma(\mathbf{r})T(\mathbf{b})\right] - \frac{N_c^2 - 1}{N_c^2} \times \right.$$
$$\left. \times \left(1 - \exp\left[-\frac{1}{2}\Sigma_2 T(\mathbf{b})\right] \right) \right\} =$$
$$= \frac{1}{2(N_c^2 - 1)} \sigma^2(\mathbf{r}) T^2(\mathbf{b}) + \ldots \quad (92)$$

Second, in the large-N_c limit, the color-octet state tends to oscillate in color remaining in the octet state. This is clearly seen from (92). Third, in the limit of an opaque nucleus,

$$\sigma_{in}(A^*(q\bar{q})_1) = \frac{1}{N_c^2} \times$$
$$\times \int d\mathbf{b} \langle \gamma^* | \left\{1 - \exp\left[-\sigma(\mathbf{r})T(\mathbf{b})\right]\right\} |\gamma^*\rangle =$$
$$= \frac{1}{N_c^2} \sigma_{in}. \quad (93)$$

This remains a constant fraction of DIS in contrast to the quasielastic diffractive DIS or inelastic diffractive excitation of a nucleus, whose cross sections vanish for an opaque nucleus [14, 36].

The analysis of the single-parton, alias single-jet, inclusive cross section is quite similar. In this case, we integrate over the momentum $\mathbf{p}_-$ of the antiquark jet such that $\mathbf{b}'_- = \mathbf{b}_-$. The corresponding matrix σ_4 has the eigenvalues

$$\Sigma_1 = \sigma(\mathbf{r} - \mathbf{r}'), \quad (94)$$

$$\Sigma_2 = \frac{N_c^2}{N_c^2 - 1} \left[\sigma(\mathbf{r}) + \sigma(\mathbf{r}')\right] - \frac{1}{N_c^2 - 1} \sigma(\mathbf{r} - \mathbf{r}') \quad (95)$$

with exactly the same eigenstates $|f_1\rangle$ and $|f_2\rangle$ as given by Eqs. (87) and (88). Again, the cross section of the

genuine inelastic DIS corresponds to the projection on the eigenstate $|f_1\rangle$, and hence

$$\frac{d\sigma_{in}}{d\mathbf{b}\,d\mathbf{p}\,dz} = \frac{1}{(2\pi)^2}\int d\mathbf{r}'d\mathbf{r}\exp[i\mathbf{p}\cdot(\mathbf{r}'-\mathbf{r})]\times$$
$$\times\,\Psi^*(Q^2,z,\mathbf{r}')\Psi(Q^2,z,\mathbf{r})\times$$
$$\times\left\{\exp\left[-\frac{1}{2}\Sigma_1 T(\mathbf{b})\right]-\exp\left[-\frac{1}{2}[\sigma(\mathbf{r})+\sigma(\mathbf{r}')]T(\mathbf{b})\right]\right\}=$$
$$=\frac{1}{(2\pi)^2}\int d\mathbf{r}'d\mathbf{r}\exp[i\mathbf{p}\cdot(\mathbf{r}'-\mathbf{r})]\times$$
$$\times\,\Psi^*(Q^2,z,\mathbf{r}')\Psi(Q^2,z,\mathbf{r})\times$$
$$\times\left\{\exp\left[-\frac{1}{2}\sigma(\mathbf{r}-\mathbf{r}')T(\mathbf{b})\right]-\right.$$
$$\left.-\exp\left[-\frac{1}{2}[\sigma(\mathbf{r})+\sigma(\mathbf{r}')]T(\mathbf{b})\right]\right\}, \quad (96)$$

which is precisely Eq. (10) in [5].

At this point, we emphasize that for the fundamental reason that the relevant final state is precisely the eigenstate $|f_1\rangle$, the calculations of the integrated inelastic cross section (89) and of the one-particle inclusive inelastic spectrum (96) are essentially Abelian problems, and the final result in (96) is identical, apart from a very different notation, to that for the propagation of relativistic positronium in dense media derived by one of the authors [32]. As can be seen from inspection of the relevant four-parton states, all contributions from the propagation of color-octet dipoles cancel, and the results can be obtained from studying the propagation of color-singlet dipoles without any reference to the full cross section matrix σ_4. Our formalism makes these cancellations nicely explicit. These quasi-Abelian problems have also been studied in [2, 38].

APPENDIX C

Weizsäcker–Williams glue of spatially overlapping nucleons

According to [5, 6], the multiple convolutions $f^{(j)}(\boldsymbol{\kappa}^2)$ have the meaning of the collective unintegrated gluon SF of j nucleons at the same impact parameter such that their Weizsäcker–Williams gluon fields overlap spatially in a Lorentz-contracted nucleus. These convolutions can also be viewed as a random walk in which $f(\boldsymbol{\kappa}^2)$ describes the single walk distribution.

To the lowest order in pQCD, the large-$\boldsymbol{\kappa}^2$ behavior is $f(\boldsymbol{\kappa}^2)\propto\alpha_S(\boldsymbol{\kappa}^2)/\kappa^4$. The phenomenological study of the differential glue of the proton in [19] suggests a useful large-$\boldsymbol{\kappa}^2$ approximation $f(\boldsymbol{\kappa}^2)\propto 1/(\boldsymbol{\kappa}^2)^\gamma$ with the exponent $\gamma\approx 2$ (a closer inspection of numerical results in [19] gives $\gamma\approx 2.15$ at $x=10^{-2}$). The QCD evolution effects enhance $f(\boldsymbol{\kappa}^2)$ at large $\boldsymbol{\kappa}^2$, the smaller x, the stronger the enhancement.

Because $f(\boldsymbol{\kappa}^2)$ decreases very slowly, we encounter a manifestly non-Gaussian random walk. For instance, as argued in [6], a j-fold walk to large $\boldsymbol{\kappa}^2$ is realized by one large walk, $\boldsymbol{\kappa}_1^2\sim\boldsymbol{\kappa}^2$, accompanied by $j-1$ small walks. We simply quote the main result in [6],

$$f^{(j)}(\boldsymbol{\kappa}^2)=jf(\boldsymbol{\kappa}^2)\left[1+\frac{4\pi^2(j-1)\gamma^2}{N_c\sigma_0\boldsymbol{\kappa}^2}G(\boldsymbol{\kappa}^2)\right], \quad (97)$$

where $G(\boldsymbol{\kappa}^2)$ is the conventional integrated gluon SF. Then the hard tail of unintegrated nuclear glue per bound nucleon,

$$f_{WW}(\mathbf{b},\boldsymbol{\kappa}^2)=\phi_{WW}(\nu_A(\mathbf{b}),\boldsymbol{\kappa}^2)/\nu_A(\mathbf{b}),$$

can be calculated parameter-free,

$$f_{WW}(\mathbf{b},\boldsymbol{\kappa}^2)=\frac{1}{\nu_A(\mathbf{b})}\sum_{j=1}^{\infty}w_j(\nu_A(\mathbf{b}))jf^{(j)}(\boldsymbol{\kappa}^2)\times$$
$$\times\left[1+\frac{4\pi^2\gamma^2}{N_c\sigma_0\boldsymbol{\kappa}^2}(j-1)G(\boldsymbol{\kappa}^2)\right]=$$
$$=f(\boldsymbol{\kappa}^2)\left[1+\frac{2\pi^2\gamma^2\alpha_S(r)T(\mathbf{b})}{N_c\boldsymbol{\kappa}^2}G(\boldsymbol{\kappa}^2)\right]. \quad (98)$$

In the hard regime, the differential nuclear glue is not shadowed; furthermore, because of the manifestly positive-valued and model-independent nuclear higher twist correction, it exhibits a nuclear antishadowing property [6].

We now present the arguments in favor of the scaling small-$\boldsymbol{\kappa}^2$ behavior

$$f^{(j)}(\boldsymbol{\kappa}^2)\approx\frac{1}{Q_j^2}\xi\left(\frac{\boldsymbol{\kappa}^2}{Q_j^2}\right)\approx\frac{1}{\pi}\frac{Q_j^2}{(\boldsymbol{\kappa}^2+Q_j^2)^2} \quad (99)$$

with

$$Q_j^2\approx jQ_0^2. \quad (100)$$

In the evolution of $f^{(j)}(\boldsymbol{\kappa}^2)$ with j at moderate $\boldsymbol{\kappa}^2$,

$$f^{(j+1)}(\boldsymbol{\kappa}^2)=\int d\mathbf{k}\,f(\mathbf{k}^2)f^{(j)}((\boldsymbol{\kappa}-\mathbf{k})^2), \quad (101)$$

the function $f(\mathbf{k}^2)$ is steep compared to the smooth and

broad function $f^{(j)}((\boldsymbol{\kappa}-\mathbf{k})^2)$, and we can therefore expand

$$f^{(j)}((\boldsymbol{\kappa}-\mathbf{k})^2) = f^{(j)}(\boldsymbol{\kappa}^2) + \frac{df^{(j)}(\boldsymbol{\kappa}^2)}{d\boldsymbol{\kappa}^2}[\mathbf{k}^2 - 2\boldsymbol{\kappa}\cdot\mathbf{k}] + \\ + \frac{1}{2}\,\frac{df^{(j)}(\boldsymbol{\kappa}^2)}{(d\boldsymbol{\kappa}^2)^2} 4(\boldsymbol{\kappa}\cdot\mathbf{k})^2 \Longrightarrow$$

$$\Longrightarrow f^{(j)}(\boldsymbol{\kappa}^2) + \mathbf{k}^2\left[\frac{df^{(j)}(\boldsymbol{\kappa}^2)}{d\boldsymbol{\kappa}^2} + \boldsymbol{\kappa}^2\frac{d^2 f^{(j)}(\boldsymbol{\kappa}^2)}{(d\boldsymbol{\kappa}^2)^2}\right] = \\ = f^{(j)}(\boldsymbol{\kappa}^2) + \mathbf{k}^2\frac{d}{d\boldsymbol{\kappa}^2}\left[\boldsymbol{\kappa}^2\frac{df^{(j)}(\boldsymbol{\kappa}^2)}{d\boldsymbol{\kappa}^2}\right], \quad (102)$$

where «$\Longrightarrow$» indicates azimuthal averaging. The expansion (102) holds for $\mathbf{k}^2 \lesssim Q_j^2$, and after the $d\mathbf{k}$ integration in (101), we obtain

$$f^{(j+1)}(\boldsymbol{\kappa}^2) = \\ = f^{(j)}(\boldsymbol{\kappa}^2) + g(j)\frac{d}{d\boldsymbol{\kappa}^2}\left[\boldsymbol{\kappa}^2\frac{df^{(j)}(\boldsymbol{\kappa}^2)}{d\boldsymbol{\kappa}^2}\right], \quad (103)$$

where

$$g(j) = \int^{Q_j^2} d\mathbf{k}\,\mathbf{k}^2 f(\mathbf{k}^2) = \frac{4\pi^2}{N_c\sigma_0}G(Q_j^2). \quad (104)$$

It is a smooth function of j. It is easy to verify that our approximation preserves the normalization condition $\int d\boldsymbol{\kappa} f^{(j)}(\boldsymbol{\kappa}^2) = 1$.

For small $\boldsymbol{\kappa}^2$ and large j, recurrence relation (104) amounts to the differential equation

$$\frac{Q_{j+1}^2 - Q_j^2}{Q_{j+1}^2 Q_j^2} = \frac{1}{Q_j^4}\frac{dQ_j^2}{dj} = -\frac{1}{Q_j^4}\frac{\xi'(0)}{\xi(0)}g(j) \quad (105)$$

with the solution

$$Q_j^2 = -\frac{\xi'(0))}{\xi(0)}\int^j dj' g(j') \approx -jg(j)\frac{\xi'(0)}{\xi(0)}. \quad (106)$$

Expansion (102) holds up to the terms proportional to $\boldsymbol{\kappa}^2$ and its differentiation at $\boldsymbol{\kappa}^2 = 0$ gives a similar constraint on the j-dependence of Q_j^2.

We note that expansion of the plateau with j entails a dilution of the differential collective glue $f^{(j)}(\boldsymbol{\kappa}^2)$ in the plateau region,

$$f^{(j)}(\boldsymbol{\kappa}^2 \lesssim Q_j^2) \propto 1/Q_j^2 \propto 1/j.$$

We conclude by the observation that when extended to $\boldsymbol{\kappa}^2 \gtrsim Q_j^2$, the parameterization in (101) and (100) behaves as $jQ_0^2/(\boldsymbol{\kappa}^2)^2$, which nicely matches the j-dependence of the leading twist term in the hard asymptotic form (99).

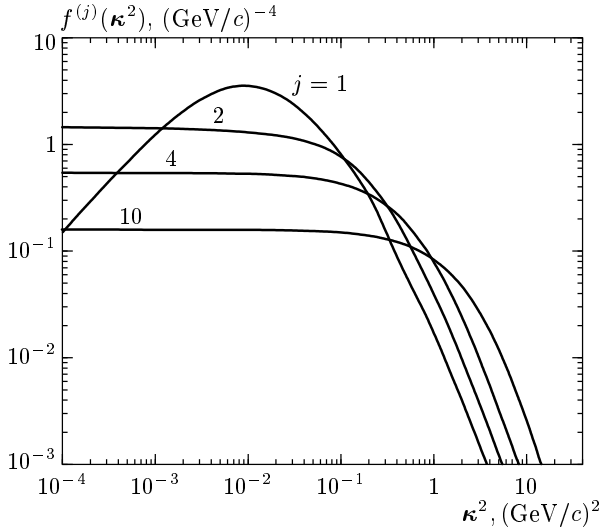

Fig. 7. The nuclear dilution for soft momenta and broadening for hard momenta of the collective glue of j overlapping nucleons, $f^{(j)}(\boldsymbol{\kappa}^2)$. The numerical results are for DIS at $x = 0.01$ and the input unintegrated gluon SF of the proton is taken from Ref. [19]

For a heavy nucleus, the dominant contribution to the expansion in (31) comes from $j \approx \nu_A(\mathbf{b})$, and hence

$$\phi_{WW}(\nu_A(\mathbf{b}), \boldsymbol{\kappa}^2) \approx \frac{1}{\pi}\,\frac{Q_A^2(\mathbf{b})}{(\boldsymbol{\kappa}^2 + Q_A^2(\mathbf{b}))^2}, \quad (107)$$

where Eq. (106) gives the width of the plateau,

$$Q_A^2(\mathbf{b}) \approx 2\nu_A(\mathbf{b})g(\nu_A(\mathbf{b})) \approx \\ \approx \frac{4\pi^2}{N_c}\alpha_S(Q_A^2)G(Q_A^2)T(\mathbf{b}). \quad (108)$$

The explicit dependence on the soft parameter σ_0 that is manifest in (104) cancels in (108). For DIS within the saturation domain, $Q^2 \lesssim Q_A^2$, the strong coupling in (33) must be taken at $r \sim 1/Q_A$, and the right-hand side of Eq. (108) exhibits only a weak dependence on the infrared parameters through the Q_A^2 dependence of the running strong coupling constant and scaling violations in the gluon SF of the nucleon. For instance, at $x = 10^{-2}$, the numerical results [19] for $G(Q^2)$ correspond to a nearly Q^2-independent $\alpha_S(Q^2)G(Q^2) \approx 1$. For the average DIS on a heavy nucleus,

$$\langle T(\mathbf{b})\rangle \approx \frac{3}{4}T(0) \approx \frac{9}{8\pi r_0^2}A^{1/3} \quad (109)$$

where $r_0 \approx 1.1$ fm. For lighter nuclei with the Gaussian density profile, $\langle T(\mathbf{b})\rangle \approx \frac{1}{2}T(0)$. Then for $N_c = 3$ and $A^{1/3} = 6$, Eqs. (108) and (109) give $\langle Q_A^2(\mathbf{b})\rangle \approx 0.8$ (GeV/c)^2.

The utility of approximation (99), (100) is illustrated in Fig. 7, where we show the j-dependence of the collective glue of j overlapping nucleons calculated for the unintegrated gluon SF of the proton from Ref. [19]. For the interaction of $q\bar{q}$ color dipoles in the average DIS on gold, ^{197}Au target, we find $\langle Q^2_{3A}(\mathbf{b})\rangle \approx 0.9$ (GeV/c)^2, in good agreement with the above estimate in Eq. (108). For the $q\bar{q}g$ Fock states of the photon, the leading $\ln Q^2$ configurations correspond to small $q\bar{q}$ pairs that act as a color-octet gluon [24]; for such gluon–gluon color dipoles, $\langle Q^2_{8A}(\mathbf{b})\rangle \approx 2.1$ (GeV/c)^2. We note in passing that the standard collinear splitting sets in, and the DGLAP evolution [34, 39] becomes applicable to the nuclear structure function, only at $Q^2 \gg \langle Q^2_{8A}(\mathbf{b})\rangle$.

REFERENCES

1. E. Leader and E. Predazzi, *Introduction to Gauge Theories and Modern Particle Physics*, Vol. 1, Cambridge University Press, Cambridge (1996); G. Sterman, *An Introduction to Quantum Field Theory*, Cambridge University Press, Cambridge (1993).

2. A. H. Mueller, Nucl. Phys. **B558**, 285 (1999);in *Lectures at the Cargèse Summer School*, August 6–18 (2001), E-print archives hep-ph/0111244.

3. A. H. Mueller, Nucl. Phys. **B335**, 115 (1990).

4. L. McLerran and R. Venugopalan, Phys. Rev. D **49**, 2233 (1994); **55**, 5414 (1997); E. Iancu, A. Leonidov, and L. McLerran, in *Lectures at the Cargèse Summer School*, August 6–18 (2001), E-print archives hep-ph/0202270.

5. N. N. Nikolaev, W. Schäfer, B. G. Zakharov, and V. R. Zoller, JETP Lett. **76**, 195 (2002).

6. N. N. Nikolaev, W. Schäfer, and G. Schwiete, Pis'ma v Zh. Eksp. Teor. Fiz. **72**, 583 (2000) [JETP Lett. **72**, 583 (2000); Phys. Rev. D **63**, 014020 (2001).

7. L. N. Lipatov, Sov. J. Nucl. Phys. **23**, 338 (1976); E. A. Kuraev, L. N. Lipatov, and V. S. Fadin, Sov. Phys. JETP **44**, 443 (1976); **45**, 199 (1977); Ya. Ya. Balitsky and L. N. Lipatov, Sov. J. Nucl. Phys. **28**, 822 (1978).

8. I. P. Ivanov, N. N. Nikolaev, W. Schäfer, B. G. Zakharov, and V. R. Zoller, in *Proceedings of 36th Annual Winter School on Nuclear and Particle Physics and 8th St. Petersburg School on Theoretical Physics*, St. Petersburg, Russia, 25 Feb.–3 Mar (2002), E-print archives hep-ph/0212161.

9. I. P. Ivanov, N. N. Nikolaev, W. Schäfer, B. G. Zakharov, and V. R. Zoller, Invited talk at the *NATO Advanced Research Workshop on Diffraction 2002*, Alushta, Ukraine, 31 Aug.–6 Sept. (2002), E-print archives hep-ph/0212176; in *Proceedings of the Workshop on Exclusive Processes at High Momentum Transfer*, Jefferson Lab., May 15–18 (2002), ed. by A. Radyushkin and P. Stoler, World Sci. Publ. (2002), p. 205; in *Proceedings of the Conference on Quark Nuclear Physics (QNP'2002)*, June 9–14, Jülich, Germany, ed. by C. Elster and Th. Walcher, Eur. Phys. J. (2003) in print, E-print archives hep-ph/0209298; Plenary talk at the *International Symposium on Multiparticle Dynamics* (ISMD'2002), Alushta, Ukraine, 8–14 Sept. (2002), ed. by G. Kozlov and A. Sissakian, World Sci. Publ. (2003), in print.

10. T. Ahmed et al. (H1 Collaboration), Nucl. Phys. B **445**, 195 (1995).

11. A. Szczurek, N. N. Nikolaev, W. Schäfer, and J. Speth, Phys. Lett. B **500**, 254 (2001).

12. J. R. Forshaw and R. G. Roberts, Phys. Lett. **335B**, 494 (1994); A. J. Askew, D. Graudenz, J. Kwiecinski, and A. D. Martin, Phys. Lett. **338B**, 92 (1994); J. Kwiecinski, A. D. Martin, and A. M. Stasto, Phys. Lett. **459B**, 644 (1999).

13. N. N. Nikolaev and B. G. Zakharov, Z. Phys. C **49**, 607 (1991).

14. N. N. Nikolaev, B. G. Zakharov, and V. R. Zoller, Z. Phys. A **351**, 435 (1995).

15. V. Barone, M. Genovese, N. N. Nikolaev, E. Predazzi, and B. G. Zakharov, Z. Phys. C **58**, 541 (1993).

16. N. N. Nikolaev and V. I. Zakharov, Yad. Fiz. **21**, 434 (1975) [Sov. J. Nucl. Phys. **21**, 227 (1975)]; Phys. Lett. **55B**, 397 (1975).

17. N. N. Nikolaev, G. Piller, and B. G. Zakharov, JETP **81**, 851 (1995); Z. Phys. A **354**, 99 (1996).

18. B. G. Zakharov, JETP Lett. **63**, 952 (1996); **65**, 615 (1997); Phys. Atom. Nucl. **61**, 838 (1998).

19. I. P. Ivanov and N. N. Nikolaev, Yad. Fiz. **64**, 813 (2001) [Phys. Atom. Nucl. **64**, 753 (2001)]; Phys. Rev. D **65**, 054004 (2002).

20. C. Adler, et al. (STAR Collaboration), Phys. Rev. Lett. **90**, 082302 (2003).

21. R. J. Glauber, in *Lectures in Theoretical Physics*, Vol. 1, ed. by W. E. Brittin et al., Intersci. Publ., Inc., New York (1959), p. 315.

22. V. N. Gribov, Zh. Eksp. Teor. Fiz. **56**, 892 (1969) [Sov. Phys. JETP **29**, 483 (1969) 483].

23. N. N. Nikolaev and B. G. Zakharov, Z. Phys. C **53**, 331 (1992).

24. N. N. Nikolaev and B. G. Zakharov, Zh. Eksp. Teor. Fiz. **105**, 1498 (1994) [JETP **78**, 806 (1994)]; Z. Phys. C **64**, 631 (1994).

25. N. N. Nikolaev, B. G. Zakharov, and V. R. Zoller, JETP Lett. **59**, 6 (1994).

26. N. N. Nikolaev and B. G. Zakharov, Phys. Lett. **332B**, 184 (1994).

27. V. Barone, M. Genovese, N. N. Nikolaev, E. Predazzi, and B. G. Zakharov, Phys. Lett. **326B**, 161 (1994).

28. B. Andersson et al. (Small-x Collaboration), Eur. Phys. J. C **25**, 77 (2002).

29. M. Genovese, N. N. Nikolaev, and B. G. Zakharov, Zh. Eksp. Teor. Fiz. **108**, 1155 (1995) [JETP **81**, 633 (1995)].

30. C. Adloff et al. (H1 Collab.), Z. Phys. C **76**, 613 (1997).

31. J. Breitweg et al. (ZEUS Collaboration), Europ. Phys. J. C **6**, 43 (1999).

32. B. G. Zakharov, Yad. Fiz. **46**, 148 (1987) [Sov. J. Nucl. Phys. **46**, 92 (1987)].

33. N. N. Nikolaev, J. Speth, and B. G. Zakharov, Zh. Eksp. Teor. Fiz. **109**, 1948 (1996) [JETP **82**, 1046 (1996)].

34. Yu. L. Dokshitser, Zh. Eksp. Teor. Fiz. **73**, 1216 (1977) [Sov. Phys. JETP **46**, 641 (1977)]; Yu. L. Dokshitzer, D. Diakonov, and S. I. Troian, Phys. Rep. **58**, 269 (1980).

35. T. Sjöstrand et al., Comp. Phys. Commun. **135**, 238 (2001).

36. V. R. Zoller, Z. Phys. C **51**, 659 (1991); M. A. Faessler, Z. Phys. C **58**, 567 (1993).

37. T. Akesson et al. (HELIOS Collab.), Z. Phys. C **49**, 355 (1991).

38. U. A. Wiedemann, Nucl. Phys. B **582**, 409 (2000).

39. V. N. Gribov and L. N. Lipatov, Sov. J. Nucl. Phys. **15**, 438 (1972); L. N. Lipatov, Sov. J. Nucl. Phys. **20**, 181 (1974); G. Altarelli and G. Parisi, Nucl. Phys. B **126**, 298 (1977).